공학박사학위논문

궤적의 모양 및 속도분포를 고려한 4절링크 최적 설계 방법론

An Optimal design method of a four-bar linkage considering shape and velocity distribution of trajectory

2017년 2월

서울대학교 대학원

기계항공공학부

김 종 원

Abstract

Four-bar linkage is one of the most versatile and useful mechanical devices. It is used as a transmission device like film advance mechanism or mechanical structure such as watt's linkage. Because the shapes of the output motion are various though the input is a simple rotary motion, the four-bar linkage as a transmission device has high utilization. Nevertheless, research about the shape and velocity of trajectory synthesis, that figure out the four-bar linkage when the desired shape and velocity of trajectory is given, is very limited. This dissertation presents a new optimal design methodology for the shape and velocity of trajectory synthesis of four-bar linkage.

This dissertation is composed of two parts. The first part contains the development of a new design method for the shape and velocity of trajectory synthesis of four-bar linkage. The second part contains the practical applications of the proposed method. The method proposed in the first part consists of three steps. In the first step, the algorithm checks whether or not the shape of the generated trajectory of four-bar linkage belongs to the desired shape category. In this dissertation, we set a hypothesis that the trajectory of crank-rocker four-bar linkage is classified into four categories, and verified it. After the generated trajectory is passed the first step, the shape of trajectory is determined in the second step. The shape of the trajectory is obtained by minimizing the root mean square error (RMSE) between the slope (first-order derivative) of the generated trajectory and that of the target trajectory. At the final step, the size of the trajectory is then determined by minimizing the RMSE between the change in angle of slope (second-order derivative) of the generated trajectory and that of the desired trajectory. This proposed approach has three advantages: i) the desired trajectory can be set as a continuous and closed loop, ii) using the desired shape category, the optimal solution can be obtained without the possibility of generating a mechanism with an unintended coupler curve, and iii) the method can take account of the velocity of the output for each section with a constant input velocity.

Because the design method of this dissertation is numerical method, the

optimization algorithm to figure out the optimal link lengths of the four-bar linkage is required. In this research, the new hybridization optimization algorithm is also presented. The algorithm is called hybrid Taguchi-random coordinate search algorithm (HTRCA). The HTRCA combines two algorithms of the Taguchi method (TM) and the random coordinate search algorithm (RCA). The RCA adjusts one variable simultaneously with two directions and various step sizes in random order to escape a local minimum. Since the RCA modifies one variable at a time according to the random order, the result of the RCA is sensitive to an initial condition of variables. The TM was adopted to generate nearly optimal initial conditions. Using the TM, the approximate optimal value can be found in even multi-modal functions. Also, the TM is used with different setting values to escape a local minimum point by changing two or more variables in one step. By combining the two methods, a global optimal value can be found efficiently. Seven test functions were optimized and the robust and efficient performance was verified by comparison with other hybrid optimization algorithms. Finally, conventional path synthesis (not the proposed path synthesis) of four-bar linkage is done by the developed optimization algorithm, and the result is compared to previous works on the same problem with evolutionary algorithms.

Three case studies were conducted to verify the advantages of the new design methodology with HTRCA based on a new index called the goodness of traceability.

The practical application of the proposed method is presented in the second part of the dissertation. That is rotational transmission mechanism for the automatic tool changer of the tapping machine. The mechanism is based on the ducal four-bar linkages. One four-bar linkage start the contact with output plate, the other four-bar linkage loses contact. To doing so, the output plate can rotate continuously. The proposed mechanism is totally different from the mechanism using single four-bar linkage the motion of which is intermittent. In case of the rotational transmission mechanism using single four-bar linkage, the shape of the trajectory is the only thing to be considered. However, in case of dual four-bar linkage, both the shape and the velocity of the contact and non-contact paths of the trajectory are considered. In this part, the design methodology, for the new rotational transmission mechanism using

the method proposed in the first part, is proposed. The design is mainly based on kinematic and singularity analysis and optimization. Dynamic simulation and prototype results are given for validation. Finally, the mechanism is applied to the tapping machine. From this case study, I conclude that the proposed methodology can be adopted to many engineering problems to figure out the four-bar linkage when the desired trajectory is given.

Keyword : Design methodology, Four-bar linkage, Mechanism design, Hybrid optimization method, Derivative-free optimization.

Student Number : 2014-30345

Table of Contents

ABSTRACT ..... **I**

PART 1 A NEW OPTIMAL DESIGN METHODOLOGY FOR SHAPE AND VELOCITY OF TRAJECTORY SYNTHESIS OF FOUR-BAR LINKAGE 1

Chapter 1. Introduction 2

1.1. Study Background 2

1.2. Recent research trend 4

1.2.1 Optimizing a multi-objective function [45] 4

1.2.2 Develop a new objective function [46] 5

1.3. Purpose and Contribution of Research 6

Chapter 2 New design methodology of a four-bar linkage 9

2.1. Classification of trajectories of crank-rocker four-bar linkage coupler point 9

2.1.1. Motivation: unintended shape generation 9

2.1.2. Classification methodology 10

2.1.3. Geometrical characteristics of each type of trajectory 12

2.1.4. Classification results and discussion 14

2.2. New design methodology of a four-bar linkage 15

2.2.1. Geometrical meaning of first-order derivative (slope) of coupler point 18

2.2.2. Geometrical meaning of second-order derivative (change in angle of slope) of coupler point 19

Chapter 3 New optimization algorithm 21

3.1. Introduction 21

3.2. Taguchi method 23

3.3. Random coordinate search algorithm 25

3.4. Hybrid Taguchi-random coordinate search algorithm (HTRCA) 26

3.5. Verification of HTRCA 28

3.5.1 Find the global optimum by test function analysis 28

3.5.1.1 Test functions 28

3.5.1.2 Results and comparison 30

3.5.2 Path synthesis of four-bar linkage 31

3.5.2.1 Case study 1: liner motion without prescribed timing 32

3.5.2.2 Case study 2: path generation with prescribed timing 32
3.5.2.3 Case study 3: path generation without prescribed timing 32
3.5.2.4 Optimization and results 33
3.5.3 Discussion 37
3.6. Conclusion 38
Chapter 4 Verification and applications 39
4.1. Case studies 39
4.1.1 Case 1–1: type-I (equal intervals) 39
4.1.2 Case 1–2: type-I (variable intervals) 40
4.1.3 Case 2–2: type-III (variable intervals) 40
4.1.4 Case 3: Avoiding intersectional shapes 41
4.2. Comparative results and discussion 42
4.2.1 Goodness of traceability(GT) index for objective comparison 42
4.2.2 The result and discussion 42
4.3. Conclusion 47
Chapter 5 Conclusion 48
PART 2 PRACTICAL APPLICATION 49
Chapter 1 Introduction 50
Chapter 2 Mechanism synthesis 52
2.1 Design concept 52
2.2 Four-bar linkage synthesis 53
2.2.1 Design objective 53
2.2.2 Synthesis of four-bar linkage 54
2.3 Rotational transmission mechanism synthesis 55
Chapter 3 Analysis 57
3.1 Analysis by simulations 57
3.1 Singularity based design selection 58
Chapter 4 Prototyping & Experiment 60
4.1 Prototyping 60
4.2 Experiment and Results 61
Chapter 5 Discussion & Conclusion 63
CONCLUSIONS AND FUTURE WORKS 65
BIBLIOGRAPHY 68
APPENDIX 1 COUPLER POINT OF CRANK-ROCKER FOUR-BAR LINKAGE 72
ABSTRACT IN KOREAN 74

List of the Tables

Table 1 Geometrical properties of each shape type 13
Table 2 Classification results 14
Table 3 $L_9(3^4)$ orthogonal array 24
Table 4 Numerical results of average 25 trials (the proposed HTRCA). 30
Table 5 Numerical results of average 25 trials (the RCA) 31
Table 6 Numerical results of average 25 trials (the algorithm in Reference [37]) 31
Table 7 Parameter setting of the HTRCA in path synthesis 33
Table 8 Comparative results for case 1. 34
Table 9 Comparative results for case 2. 35
Table 10 Comparative results for case 3. 36
Table 11 Comparative results of case 1 43
Table 12 Comparative results of case 2 and 3 43
Table 13 The results of path synthesis of four-bar linkage 54
Table 14 Fluctuations of angular velocity of output plate 57
Table 15 Required input torque of four-bar linkage 58
Table 16 Minimum values of $\theta 4$ 59

List of the Figures

Figure 1 (Left) Film advance mechanism [1], (Right) Watt's linkage suspension of train [2] 2
Figure 2 (Left) Atlas of Four-bar linkage [3], (Right) Drawing by hands [12] 3
Figure 3 The result of the research [45] 5
Figure 4 Equal error lines for CMDE function [46] 5
Figure 5 The optimal design according to the weighting factor (=F) [46] 6
Figure 6 The result of a case study for tracing human gait trajectory obtained by motion capture 10
Figure 7 Categories of the trajectories of crank-rocker four-bar linkage: (a) Type-I (ellipse shape), (b) Type-II (semi-ellipse shape), (c) Type-III (crescent-like shape), (d) Type-IV (Intersectional shape). 11
Figure 8 To facilitate the distinguishing of shapes, the obtained trajectory was rotated by θrot to have the maximum width 11
Figure 9 Infinite points and zero-slope point of each type of trajectories 13
Figure 10 Exceptional cases of the classification of trajectory 15
Figure 11 The new path synthesis for the design of four-bar linkage 17
Figure 12 Diagram for the proof of PROPOSITION 1 19
Figure 13 Random coordinate search algorithm 25
Figure 14 HTRCA for global optimization problem 27
Figure 15 Coupler curves obtained in Case 1 34
Figure 16 Coupler curves obtained in Case 2 35
Figure 17 Coupler curves obtained in Case 3 36
Figure 18 Desired trajectories of case study (A) Case 2 (B) Case 3 40
Figure 19 Simulation result of case 1 (ellipse shape) 44
Figure 20 Simulation result of case 2 (crescent-like shape) 45
Figure 21 Simulation result of case 3 (walking motion) 45
Figure 22 Four-bar linkage mechanism of case study 1(Input link: blue link) 46
Figure 23 Four-bar linkage mechanism of case study 2(Input link: blue link) 46
Figure 24 Four-bar linkage mechanism of case study 3(Input link: blue link) 47
Figure 25 Design concept of the new rotational transmission mechanism 52
Figure 26 Statistical analysis of crescent-like shape of the trajectory and design objective of the four-bar linkage trajectory 53
Figure 27(Left) Schematic of four-bar linkage and (Right) crescent-like shape trajectory with geometrical properties 54
Figure 28 Design procedure of rotational transmission mechanism 55
Figure 29 Rotational transmission mechanisms of each case 56
Figure 30 Angular velocity of output plate by simulation 58
Figure 31 The prototype of the RTM for the automatic tool changer. Posture during (1-6) counterclockwise motion 60

Figure 32 The prototype of ATC using RTM 60
Figure 33(Left) The experimental environment and (Right) Rotary encoder to measure an angular velocity of output plate 61
Figure 34 The angular velocity of output plate 61
Figure 35 The angle of the output from the second experiment 61

Part 1

A new optimal design methodology for shape and velocity of trajectory synthesis of four-bar linkage

Chapter 1. Introduction

1.1. Study Background

A four-bar linkages are widely used in mechanical devices due to their simple structure, ease of manufacturing, and versatility. The use of the four-bar linkage can be classified into two categories. First, because of a wide variety of the output motions of the four-bar linkage though the input motion is a simple rotary motion, the four-bar linkage is used as a transmission device. One example is a film advance mechanism [1] of projector. The mechanism can transmission the rotary input motion to linear motion for the advance of a frame of the film. Second, due to the capability of force dispersion and compliance, the four-bar linkage also used as the mechanical structure. Watt's linkage [2] is a typical example.

The research about the path synthesis of planar four-bar linkage, that figuring out the proper four-bar linkage when the desired output motion is given, has been studied with a variety of methods during the past 60 years [3 -9]. The methods in these studies can be classified as graphical, analytical, or numerical method.

Hrones and Nelson used a graphical method that involves an atlas of coupler curves [3]. They developed a four-bar linkage atlas with almost 7000 coupler curves. Similarly, Zhang et al. [10] proposed an atlas of five-bar geared linkage coupler curves. Alternatively, other graphical methods involve drawing by hand [11, 12]. Graphical methods are quick and straightforward, but the accuracy of these

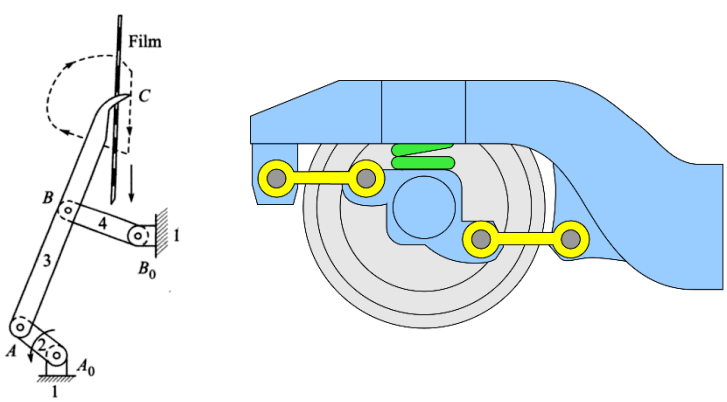

Figure 1 (Left) Film advance mechanism [1], (Right) Watt's linkage suspension of train [2]

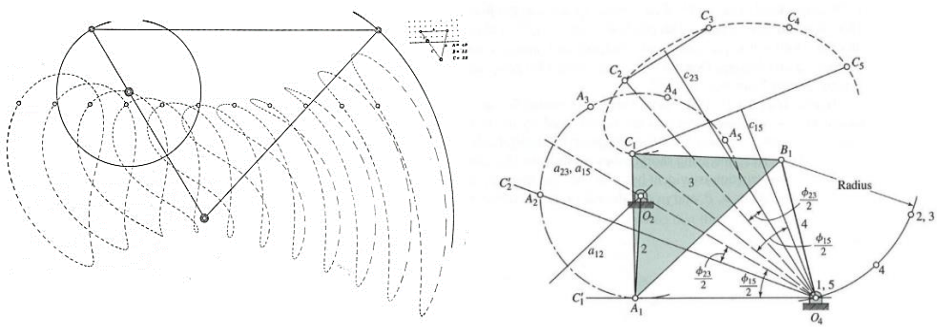

Figure 2 (Left) Atlas of Four-bar linkage [3], (Right) Drawing by hands [12]

approaches is limited due to drawing error, which can be critical for the design of precision mechanical devices. Also, because of the complexity of obtaining solutions with a reasonable result, the geometric construction may have to be repeated many times.

Analytical approaches were first addressed by Sandor [4] and by other researchers thereafter [13,14]. Methods for finding suitable four-bar linkages that can precisely trace desired precision points analytically have been developed, and the number of desired precision points has increased from four to nine. Once a mechanism is modeled mathematically and coded for a computer simulation, parameters such as the lengths of each link are easily handled to create new solutions without further programming. However, there is no analytical solution to the general problem of four-bar linkage synthesis for more than nine target points. Thus, this methodology cannot be applied for the design of four-bar linkages whose coupler point can trace a large number of target points or continuous and closed loops. This problem may be solved using a numerical method.

There are two types of numerical method. One is using numerical atlas database of coupler curve with Fourier series method [15,16,17]. The other method is optimizing parameters to minimize an objective function, and obtain the solution numerically. Because it can be used for more than nine target points and ease of calculation, the numerical method is commonly used for the design of four-bar linkage. The most widely used objective function is the tracking error (TE), which is defined as the sum of the square of the Euclidean distance between the desired points and the obtained coupler points described as follows

$$f_{obj} = \sum_{i=1}^{N} \left[\left(C_{xd}^{i} - C_{x}^{i}(X) \right)^2 + \left(C_{yd}^{i} - C_{y}^{i}(X) \right)^2 \right] \quad (1)$$

where $C_{xd}^{i},\ C_{yd}^{i}$: i^{th} desired point

$C_{x}^{i}(X),\ C_{y}^{i}(X)$: i^{th} generated point with design variable X

To the best of our knowledge, the first to address this objective function was Han [5]. Because it can be used for more than nine target point and ease of calculation, TE has been used in various studies [7,18,19]. Therefore, the numerical method is the most reasonable choice from the three (graphical, analytical and numerical) methods. However, using TE for the objective function could generate unintended trajectory shapes. Furthermore, when the input angular velocity is constant, it is not easy to take account of the velocity of the coupler point that traces the trajectory of the four-bar linkage.

1.2. Recent research trend

Due to the growth of the computer performance and the complexity of required trajectory of the four-bar linkage, the research about the numerical method to figure out the optimal design of four-bar linkage has been conducted recently. Some of them are introduced in this section.

1.2.1 Optimizing a multi-objective function [45]

One of the research trends to figure out the proper four-bar linkage is proposing a multi-objective function and optimizing it. Nariman-Zadeh et al.,[45] proposed the multi-objective function which is composed of the tracking error(TE) and transmission angle error(TA) which is defined as transmission angle's deviation from 90°. The transmission angle error (TA) is computed as the sum of the square of the maximum deviations of the transmission angle γ of the mechanism for the whole path and is given by

$$\text{TA} = \left[\left(\gamma_{max} - 90^{\circ} \right)^2 + \left(\gamma_{min} - 90^{\circ} \right)^2 \right]$$

It can be seen that the ideal value of this objective function is zero when both the

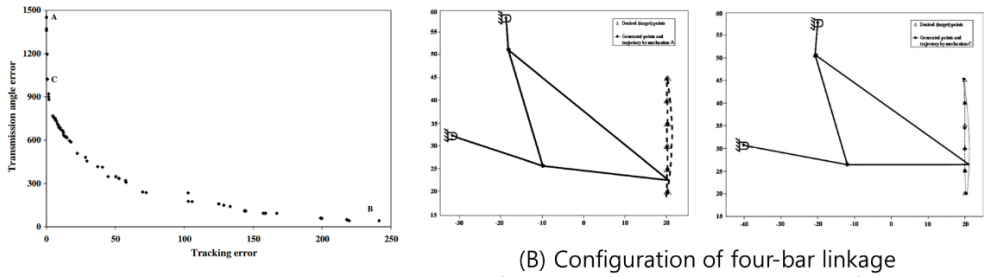

(A) Optimization results

(B) Configuration of four-bar linkage
(left) result of point A (right) result of point C

Figure 3 The result of the research [45]

maximum and the minimum values of the transmission angle γ are 90° during the entire trajectory.

From the pareto optimum synthesis of four-bar mechanism demonstrated in Fig. 3, the authors present the optimal solutions of the line trajectory to minimize the multi-objective function. Because the TA means power transmission efficiency, if the four-bar linkage is design for power transmission, the proposed method has an advantages compared to the other method. However, the TA and TE are in inverse proportion to each other demonstrated in Fig. 3. Therefore, the designer has to find proper the weighting factor of each objective values for their design problem.

1.2.2 Develop a new objective function [46]

The other trend of the design of four-bar linkage is present a new objective function. Matekar et al., [46] proposed a new objective function called 'Cumulative Modified Distance Error function(CMDE)' described as follows:

$$\text{CMDE} = \sum_{i=1}^{n} e_{mi}$$

$$e_{mi} = Fe_{ti} + e_{li}$$

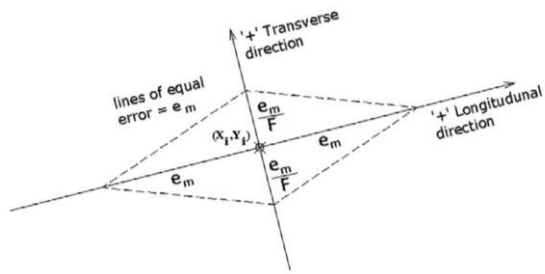

Figure 4 Equal error lines for CMDE function [46]

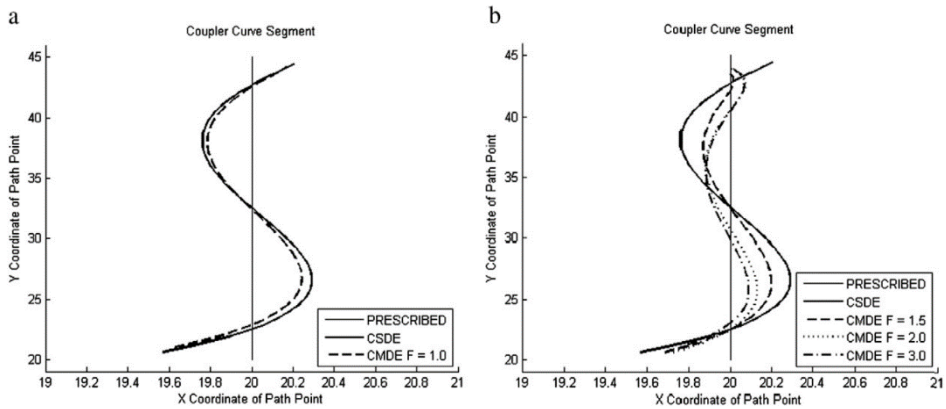

Figure 5 The optimal design according to the weighting factor (=F) [46]

As demonstrated in Fig. 5, the proposed objective function provides the designer with an alternate option as far as the choice of error function is concerned.

1.3. Purpose and Contribution of Research

Despite the research about the numerical method have been conducted actively, the research about the method can consider the shape and velocity simultaneously or overcome the disadvantage that generating unintended shape of trajectory is limited. Therefore, the optimal design method for shape and velocity of trajectory of four-bar linkage is proposed.

The new optimal design method consists of three steps. In the first step, the algorithm checks whether or not the shape of the generated trajectory of four-bar linkage belongs to the desired shape category. We set a hypothesis that the trajectory of crank-rocker four-bar linkage is classified into four categories, and verified it. After the generated trajectory is passed the first step, the shape of trajectory is determined in the second step. The shape of the trajectory is obtained by minimizing the root mean square error (RMSE) between the slope (first-order derivative) of the generated trajectory and that of the target trajectory. At the final step, the size of the trajectory is then determined by minimizing the RMSE between the change in angle of slope (second-order derivative) of the generated trajectory and that of the desired trajectory.

This method has three advantages compared to conventional numerical approaches. First, using the derivative of the trajectory, which is a continuous

function, the desired trajectory can be set as a continuous and closed loop. In contrast, methods that minimize TE require points for the desired trajectory. Second, if the four-bar linkage is designed to follow the derivative value profile according to the input angle, the method can obtain the optimal solution without the possibility of generating an unintended shape. Finally, by adjusting the interval of two peak points of the derivative profile of the desired trajectory, the method can take account of the velocity of each section of the coupler curve with constant input velocity.

Because the developed method of this part is numerical method, the optimization algorithm to figure out the optimal link lengths of the four-bar linkage is required. In this research, the new hybridization optimization algorithm also presented. The algorithm is called hybrid Taguchi-random coordinate search algorithm (HTRCA). The HTRCA combines two algorithms of the Taguchi method (TM) and the random coordinate search algorithm (RCA). The RCA adjusts one variable simultaneously with two directions and various step sizes in random order to escape a local minimum. Since the RCA modifies one variable at a time according to the random order, the result of the RCA is sensitive to an initial condition of variables. The TM was adopted to generate nearly optimal initial conditions. Using the TM, the approximate optimal value can be found in even multi-modal functions. Also, the TM is used with different setting values to escape a local minimum point by changing two or more variables in one step. By combining the two methods, a global optimal value can be found efficiently. Seven test functions were optimized and the robust and efficient performance was verified by comparison with other hybrid optimization algorithms. Finally, conventional path synthesis (not the proposed method) of four-bar linkage is done by the developed optimization algorithm, and the result is compared to previous works on the same problem with evolutionary algorithms.

Three case studies were conducted to verify the advantages of the new methodology based on a new performance index called the goodness of traceability. From the many case studies, we conclude that the proposed method can be adopted to many engineering problems to figure out the four-bar linkage when the desired trajectory is given.

Part 1 of dissertation is organized as follows. The new method of planer four-bar linkage is introduced in **Chapter 2**. Then the optimization algorithm for the

design method and its verification are presented in **Chapter 3**. The verification of the proposed design methodology with optimization algorithm mentioned in chapter 2 are demonstrated in **Chapter 4**. Finally, the conclusion of this part is given in **Chapter 5**.

Chapter 2 New design methodology of a four-bar linkage

In this chapter, the new design methodology of a four-bar linkage as numerical method is proposed. The design methodology consists of three steps. In the first step, the algorithm checks whether or not the shape of the generated trajectory of four-bar linkage belongs to the desired shape category. We set a hypothesis that the trajectory of crank-rocker four-bar linkage is classified into four categories, and verified it. After the generated trajectory is passed the first step, the shape of trajectory is determined in the second step. The shape of the trajectory is obtained by minimizing the root mean square error (RMSE) between the slope (first-order derivative) of the generated trajectory and that of the target trajectory. At the final step, the size of the trajectory is then determined by minimizing the RMSE between the change in angle of slope (second-order derivative) of the generated trajectory and that of the desired trajectory.

The details of the design methodology are explained in this chapter. And the advantages and verification of the method will be explained in the chapter 4.

2.1. Classification of trajectories of crank-rocker four-bar linkage coupler point

2.1.1. Motivation: unintended shape generation

When designing a four-bar linkage that can trace a target trajectory by minimizing TE, unintended shapes of the coupler curve can sometimes be obtained, as shown in Fig. 6. To avoid this, we set the hypothesis that the trajectory of crank-rocker four-bar linkage is classified into several categories. For example, the solution for the desired trajectory demonstrated in Fig. 6, which is part of the “non-intersectional shape” category, would not normally be obtained.

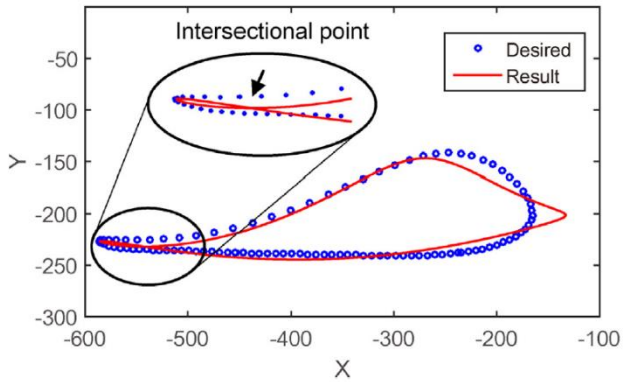

Figure 6 The result of a case study for tracing human gait trajectory obtained by motion capture

2.1.2. Classification methodology

Through the experience of observing the trajectory of four-bar linkage, we set the hypothesis that the trajectory of crank-rocker four-bar linkage is classified into four categories shown in Fig.7. The ellipse-like shape is Type-I, the shape that includes linear motions is Type-II, the crescent-like shape is Type-III, and the shape that has an intersection point is Type-IV. Two methods were used to validate this classification. The first method is visual inspection of the coupler curves of the atlas by Hrones and Nelson [3]. Approximately 7,000 coupler curves were categorized. This method does not need further work such as coding, so it is easy and simple to apply this method to the atlas. However, because visual inspection is done with the human eye, the accuracy and reproducibility of the result may low.

The second method is generating link lengths of a four-bar linkage randomly and checking whether or not each trajectory belongs to one of the four types using the geometrical characteristics of each type. Over 100,000 coupler curves were examined. Since the shape is the only thing to be considered in the classification, the generated trajectories were rotated to have the maximum width, as shown in Fig. 8. We found a vector which has maximum length in the trajectory, and rotated the trajectory by the slope of the vector relative to the origin point. After rotating the trajectory, the geometrical characteristics were considered. The details are described in the next section. Once the geometrical features are coded for a computer simulation, it is easy to classify a large number of coupler curves. The simulation also enables very high accuracy and reproducibility of the results compared to visual

inspection. However, the geometrical characteristics are needed, and programing takes more time.

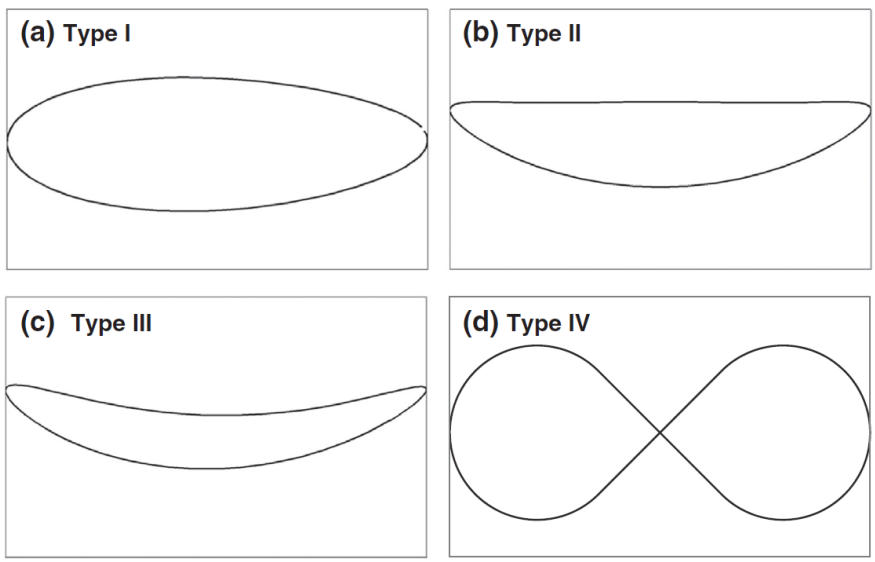

Figure 7 Categories of the trajectories of crank-rocker four-bar linkage: (a) Type-I (ellipse shape), (b) Type-II (semi-ellipse shape), (c) Type-III (crescent-like shape), (d) Type-IV (Intersectional shape).

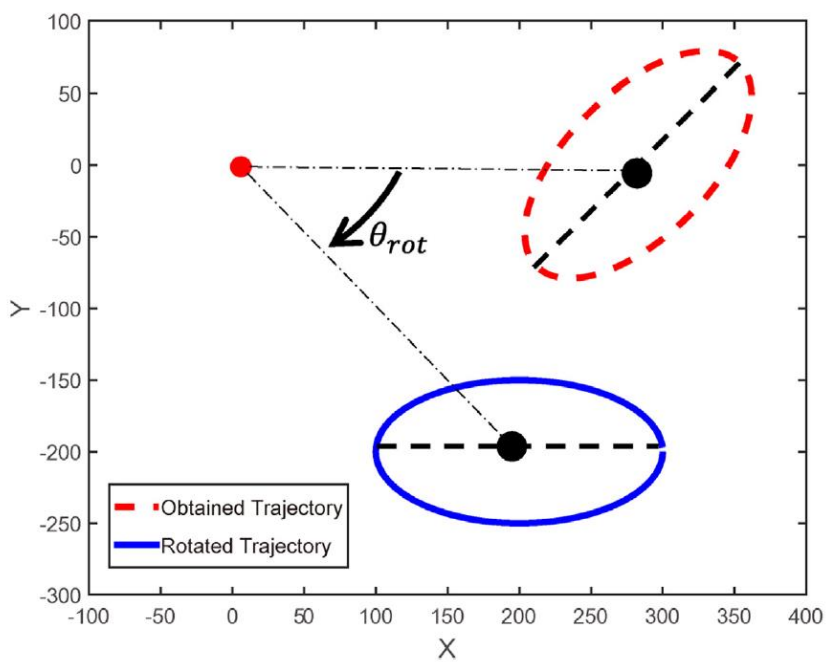

Figure 8 To facilitate the distinguishing of shapes, the obtained trajectory was rotated by θ_{rot} to have the maximum width

2.1.3. Geometrical characteristics of each type of trajectory

The geometrical characteristics that distinguish each shape type are the first-order and second-order derivatives of the coupler curve of a four-bar linkage and the radius of curvature of some sections of the trajectory. These characteristics are described as follows:

First-order derivative (slope):

$$\frac{\partial C_y}{\partial C_x} = \frac{\partial C_y}{\partial \theta_1}\frac{\partial \theta_1}{\partial C_x} \tag{2a}$$

Second-order derivative (change in angle of slope):

$$\frac{\partial^2 C_y}{\partial {C_x}^2} = \frac{\partial}{\partial C_x}\left(\frac{\partial C_y}{\partial C_x}\right) = \left(\frac{\partial C_x}{\partial \theta_1}\frac{\partial^2 C_y}{\partial {\theta_1}^2} - \frac{\partial^2 C_x}{\partial {\theta_1}^2}\frac{\partial C_y}{\partial \theta_1}\right) \Big/ \left(\frac{\partial C_x}{\partial \theta_1}\right)^3 \tag{2b}$$

Radius of curvature

$$R = \left| \left(1 + \frac{\partial {C_x}^2}{\partial C_y}\right)^{\frac{3}{2}} \Big/ \frac{\partial^2 C_x}{\partial {C_y}^2} \right| \tag{2c}$$

Where, C_x, C_y are the coupler point of four-bar linkage described in **Appendix 1**

If the derivative values are plotted according to the input angle θ_1, there are only two points at which the first-order derivative is infinite for all types. The infinite points divide the trajectory into an upper side and lower side, as demonstrated in Fig. 9. In the case of Type-I, there is one zero-slope point for each part, where the first-order derivative is zero. In addition, the sign of the second-order derivative at the zero-slope points is different for each side of the trajectory. The sign of the upper zero-slope point is negative, and that of the lower side is positive.

In Type-II, there are one or three points on the flat side and one on the other side. Since the flat side does not include a straight line, the number of zero-slope points varies from one to three. Thus, the radius of curvature is used to distinguish this type from the others. If the radius of curvature of one side is almost infinite, the shape must be classified as Type-II.

In the case of Type-III, there are three zero-slope points on one side and one on

the other side. In addition, the signs of the second-order derivative of each side are the same. Finally, in Type-IV, there are two zero-slope points per side. Table 1 gives a summary of these geometrical features.

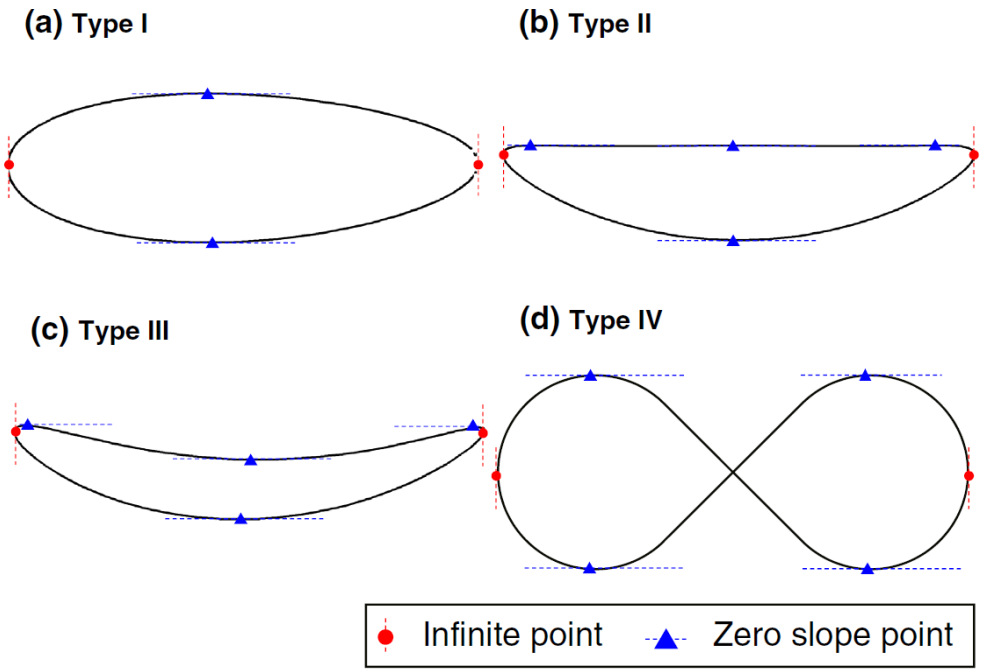

Figure 9 Infinite points and zero-slope point of each type of trajectories

Table 1 Geometrical properties of each shape type

Type		I	II	III	IV
Num. of Infinite points		2	2	2	2
Zero slope point(ZSP) ratio		1:1	1:1 or 1:3	1:3	2:2
Sign of second derivative at ZSP	Upper	-	- or +	+	+/-
	Lower	+	+	+	-/+
Radius of curvature		Finite	Infinite	Finite	Finite

2.1.4. Classification results and discussion

Using the method described in the previous section, 6889 coupler curves were examined, and the results are shown in Table 2. Among the coupler curves of the atlas, Type-I elliptical shapes account for 59.22% of the total coupler curves. Types-II, III, and IV account for 10.77%, 21.55%, and 8.36%, respectively. 0.1% of all coupler curves cannot be categorized into one of the four types. In particular, two of them had an elliptical shape, but there were five zero-slope points on one side. Another one had an intersectional shape, but the number of zero-slop points was the same as Type III. Thus, these exceptional cases have two intersectional points.

Similar results can be observed with the second methodology. A total of 10,165 coupler curves were examined using the second method. Among all trajectories of randomly generated four-bar linkages, Type-I accounts for 66.47%, while Types- II, III, and IV account for 5.90%, 19.69%, and 7.91%, respectively. In this case, there are only three exceptions. One is the same as the latter exception of the first method. Another case has four infinite points, and the third one has an intersectional shape, but it has four zero-slope points on one side of the trajectory. Because of the difference in the boundaries of each link length, it seems that the results of each method are slightly different. But each result shows the same trends. Despite the exceptional trajectory shapes, the results show that four shape types can cover 99.95% of all of the trajectories. The 10 exceptional cases are not enough to be considered as a single category, so they were assumed to be negligible. Some of them are demonstrated in Fig. 10.

Table 2 Classification results

	First method (visual inspection)	Second method (using geometrical features)
Type I	4,081 (0.5922)	6,757 (0.6647)
Type II	742 (0.1077)	600 (0.0590)
Type III	1,485 (0.2155)	2,001 (0.1969)
Type IV	574 (0.0836)	804 (0.0791)
Exception	7 (0.0010)	3 (0.0003)
Total	6,889 (1.0000)	10,165 (1.0000)

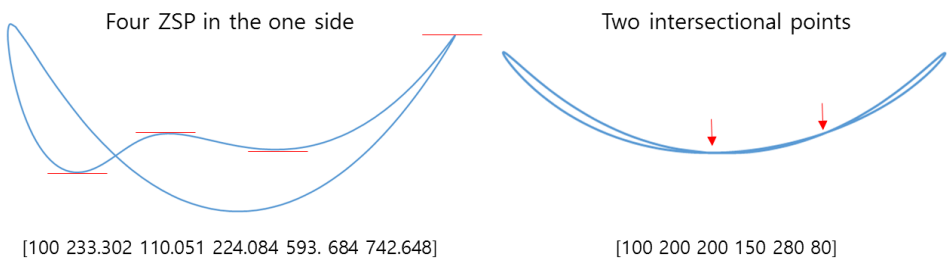

Figure 10 Exceptional cases of the classification of trajectory

The classification has two advantages compared to exist classification [20]. First, because four categories are easy to distinguish from each other, a designer can easily choose a category that involves the shape of desired trajectory by visual inspection. Second, the geometrical properties used for the classification are simple to calculate. This means that the classification process in computer simulation is so fast that if this classification is used for the design of four-bar linkage, whole design time can be reduced.

2.2. New design methodology of a four-bar linkage

To obtain an optimal trajectory numerically without the possibility of generating an unintended trajectory shape, the following three-step design methodology is developed:

Step 1.

1. Generate the design variables of four-bar linkage according to the **optimization algorithm** and find the trajectory of the four-bar linkage.
   A. Design variables from the **Step 2**(X_{link}) : $[l_2 \quad l_3 \quad l_4 \quad l_{cx} \quad l_{cy}]/l_1$
   B. Design variable from the **Step 3** : l_1
2. Check the shape of the generated trajectory whether or not belong to the desired shape category.
3. If the trajectory belongs to the desired shape category, go to the next step. Otherwise, start from the beginning again.

Step 2.

1. Calculate the objective function described as follows:

$$f_{obj(1)} = RMS\left(\frac{d}{dt}Traj._G\,(\theta_t) - \frac{d}{dt}Traj._D\,(\theta_t - \theta_0)\right)$$

Where RMS : Root-mean-square

$Traj._G$: Generated Trajectory

$Traj._D$: Desired Trajectory

θ_t : Input angle

2. Compare the objective function value to the previous evaluation.
3. If the value of $f_{obj(1)}$ is minimized according to the **optimization algorithm**, go to the next step with optimal variables $X_{link}{}^*$. Otherwise, go to the **Step 1** and start again.

Step 3.

1. Calculate the objective function described as follows:

$$f_{obj(2)} = RMS\left(\frac{d^2}{dt^2}Traj._G\,(\theta_t) - \frac{d^2}{dt^2}Traj._D\,(\theta_t - \theta_0)\right)$$

Subject to $X_{link} = X_{link}{}^*$

2. Compare the objective function value to the previous evaluation.
3. If the value of $f_{obj(2)}$ is minimized according to the **optimization algorithm**, stop the algorithm and print the optimal design variables $X^* = \left[l_1, l_2, l_3, l_4, l_{cx}, l_{cy}\right]^*$. Otherwise, go to the **Step 1** and start again.

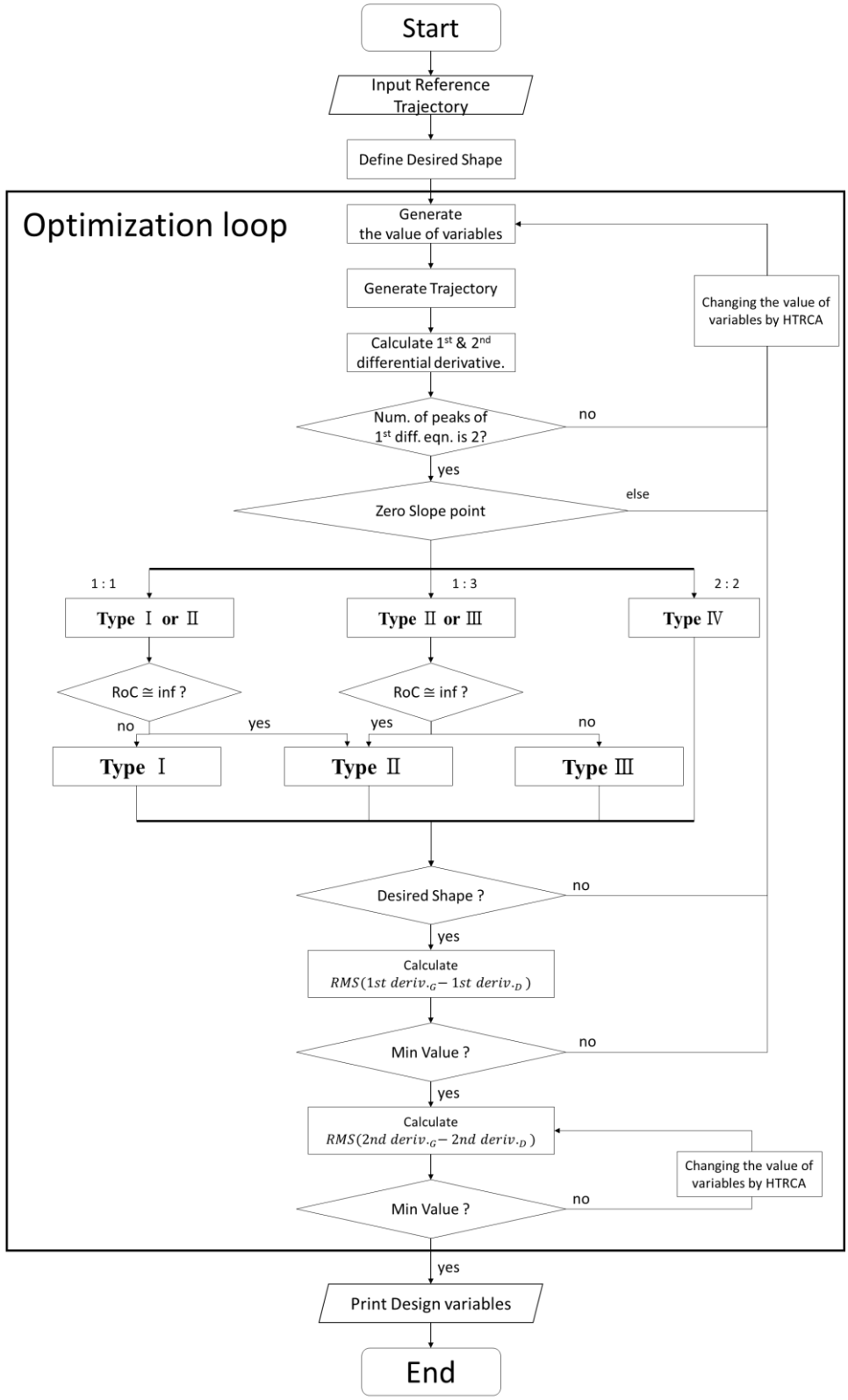

Figure 11 The new path synthesis for the design of four-bar linkage

2.2.1. Geometrical meaning of first-order derivative (slope) of coupler point

In the step 2 of the design methodology, the slope of the trajectory of the coupler curve is used to find the shape of trajectory. We propose the following geometrical interpretation of the first-order derivative of the coupler curve:

PROPOSITION 1: If two plane figures have the same first-order derivative profile, they can be called mathematically similar.

PROOF OF PROPOSITION 1:

In the discrete system and based on Fig. 12,

(1) $i = 1$

If $\varphi_{s,1} = \varphi_{b,1}$, then $\Delta O p_{s,1} p_{b,2}$ and $\Delta O p_{b,1} p_{b,2}$ are similar. The similarity ratio is $\frac{n_1 r_1}{r_1} = n_1$. The tangent values of angles $\varphi_{s,1}$ and $\varphi_{b,1}$ are described as follows:

$$\tan \varphi_{s,1} = \frac{\Delta y}{\Delta x} = \frac{r_2 \sin \theta_2 - r_1 \sin \theta_1}{r_2 \cos \theta_2 - r_1 \cos \theta_1} \tag{3a}$$

$$\tan \varphi_{b,1} = \frac{n_2 r_2 \sin \theta_2 - n_1 r_1 \sin \theta_1}{n_2 r_2 \cos \theta_2 - n_1 r_1 \cos \theta_1} \tag{3b}$$

Because $\varphi_{s,1}$ and $\varphi_{b,1}$ are assumed to be the same, equations (3a) and (3b) are the same. This implies that the similarity ratios n_1 and n_2 are the same.

(2) $i = k$

If $\varphi_{s,k} = \varphi_{b,k}$, then $\Delta O p_{s,k} p_{s,k+1}$ and $\Delta O p_{b,k} p_{b,k+1}$ are similar. The similarity ratio is $\frac{n_k r_k}{r_k} = n_k$. The tangent values of angles $\varphi_{s,k}$ and $\varphi_{b,k}$ are described as follows:

$$\tan \varphi_{s,k} = \frac{\Delta y}{\Delta x} = \frac{r_{k+1} \sin \theta_{k+1} - r_k \sin \theta_k}{r_{k+1} \cos \theta_{k+1} - r_k \cos \theta_k} \tag{4a}$$

$$\tan \varphi_{b,k} = \frac{n_{k+1} r_{k+1} \sin \theta_{k+1} - n_k r_k \sin \theta_k}{n_{k+1} r_{k+1} \cos \theta_{k+1} - n_k r_k \cos \theta_k} \tag{4b}$$

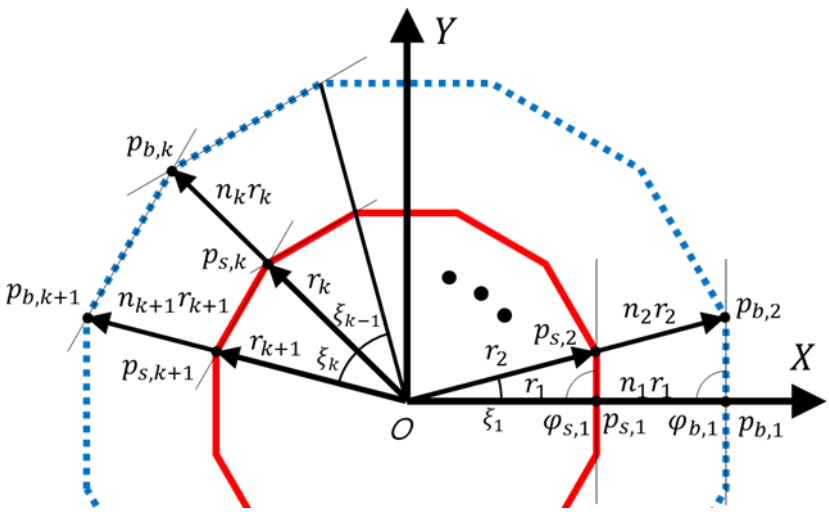

Figure 12 Diagram for the proof of PROPOSITION 1

Because $\varphi_{s,\mathrm{k}}$ and $\varphi_{b,\mathrm{k}}$ are assumed to be the same, equations (4a) and (4b) are the same. This implies that the similarity ratios n_{k} and $n_{\mathrm{k+1}}$ are the same.

By mathematical induction, the similarity ratio of step k (n_k) is the same as that of step 1 (n_1). This means that if two plane figures have the same first-order derivative in all discrete segments, they are mathematically similar. This can also be applied to a continuous system by decreasing the interval angle θ_k.

2.2.2. Geometrical meaning of second-order derivative (change in angle of slope) of coupler point

In the step 3 of the design methodology, the change in angle of slope is used to determine the size of the coupler curve. We propose the following geometrical interpretation of the derivative:

PROPOSITION 2: If two plane figures have the same first and second-order derivative profiles, they are the same figure.

PROOF OF PROPOSITION 2:

The second-order derivative value can be obtained as follows:

$$\frac{\partial^2 C_y}{\partial {C_x}^2}_{small} \sim \frac{\Delta\left({}^{\Delta y}/_{\Delta x}\right)}{\Delta x} = \frac{\tan^{-1}\varphi_{s,k+1} - \tan^{-1}\varphi_{s,k}}{r_k\left(\cos\theta_{sum(k)} - \cos\theta_{sum(k-1)}\right)} \tag{5a}$$

$$\frac{\partial^2 C_y}{\partial {C_x}^2}_{big} \sim \frac{\Delta\left({\Delta y}/{\Delta x}\right)}{\Delta x} = \frac{\tan^{-1}\varphi_{s,k+1} - \tan^{-1}\varphi_{s,k}}{n_k r_k\left(\cos\theta_{sum(k)} - \cos\theta_{sum(k-1)}\right)} \tag{5b}$$

where

$$\theta_{sum(k)} = \sum_{i=1}^{k} \theta_i$$

If the second-order derivative values of each plane figure are the same, equation (5a) is equal to equation (5b).

$$\frac{\partial^2 C_y}{\partial {C_x}^2}_{big} = \frac{1}{n_k}\frac{\partial^2 C_y}{\partial {C_x}^2}_{small} \tag{6}$$

Equation (9) shows that the similarity ratio n_k has to be one. In other words, the two plane figures are exactly the same.

Chapter 3 New optimization algorithm

Because the design methodology is numerical method, the optimization algorithm to figure out the optimal link lengths of the four-bar linkage is required. In this chapter, the new hybridization optimization algorithm is presented. The algorithm is called hybrid Taguchi-random coordinate search algorithm (HTRCA). The HTRCA combines two algorithms of the Taguchi method (TM) and the random coordinate search algorithm (RCA). The RCA adjusts one variable simultaneously with two directions and various step sizes in random order to escape a local minimum. Since the RCA modifies one variable at a time according to the random order, the result of the RCA is sensitive to an initial condition of variables. The TM was adopted to generate nearly optimal initial conditions. Using the TM, the approximate optimal value can be found in even multi-modal functions. Also, the TM is used with different setting values to escape a local minimum point by changing two or more variables in one step. By combining the two methods, a global optimal value can be found efficiently. Seven test functions were optimized and the robust and efficient performance was verified by comparison with other hybrid optimization algorithms. Finally, conventional path synthesis (not the proposed path synthesis) of four-bar linkage is done by the developed optimization algorithm, and the result is compared to previous works on the same problem with evolutionary algorithms.

3.1. Introduction

In the design methodology of four-bar linkage as a numerical method, the optimization algorithm, which can find the optimal solution of the objective function, is used. Because the optimal solution of the four-bar linkage depends strongly on the performance of the optimization algorithm, many studies, adopting the conventional algorithm or developing a new algorithm to determine the four-bar linkage, have been conducted. Despite most objective functions being defined by simple equations, due to the complexity and hardness of the calculation, it is reasonable that the objective functions used in the numerical method be treated as black box functions [23], which can only obtain the value of a function. To find the optimal solution of

the black box functions, the derivative-free optimization (DFO) algorithm was used [24]. The genetic algorithm (GA) is the most widely used DFO algorithm in engineering. Various types of GA are also used in the path synthesis of four-bar linkage [25–28]. The differential evolution (DE), simulated annealing (SA) and particle swarm optimization (PSO) are also used widely in the path synthesis of a four-bar linkage [28–31]. These methods are inspired by nature or everyday lives. Despite the high computational cost, they are easy to apply to optimization problems. On the other hand, many of them have a strong dependence on the initial condition. This suggests that the robustness of the design method is not good. Therefore, hybridized algorithms have been developed to overcome this disadvantage [25, 26, and 32]. If the two methods are hybridized, the weakness of each method is eliminated and the strengths of each method are enhanced. Therefore, the robustness of the hybridized algorithm is better than that of a single algorithm.

This chapter proposes an optimization algorithm called the hybrid Taguchi-random coordinate search algorithm (HTRCA) that combines the Taguchi Method (TM) with the modified the random coordinate search algorithm (RCA) as a tool for the design methodology of a four bar linkage. The TM is a proven and robust design method based on experimental data [33]. The method does not require the derivatives of the objective function. Using sensitivity analysis based on an orthogonal array, the TM does not require an extensive function evaluation, which is in contrast to a general DFO. On the other hand, because of the step size and the need for the operator decisions between each experiment, it is difficult to find the optimal point precisely using only the TM. The RCA is a derivative-free algorithm that is sometimes called the random coordinate descent method. The RCA can find an optimal point by optimizing a function value along one direction generated randomly one at a time. This method is simple and easy to apply to the objective function. On the other hand, it needs a considerable function evaluation and can be difficult to apply to some very complex objective functions, such as non-convex functions [34]. The HTRCA can find the optimal solution through a three step optimization. In the first step, TM is used to find a rough optimal point of a bounded objective function. The RCA is used to find a global optimal point. Finally, the TM is used again to test whether or not the point is optimal. By combining the two methods, the HTRCA obtains more reliable results than either method alone, particularly in the path

synthesis problem of a four-bar linkage. There are three strategies to escape a local optimal point in the HTRCA. First, the RCA generates search coordinates randomly. Second, if a point is suspected to be an optimal point, the step size of RCA is increased sequentially up to the maximum step size. Third, if the point passes the optimal test, it is tested again by TM. Because TM modifies more than one coordinate, it provides a chance to escape the local optimal points.

The aims of this chapter are to propose a new hybridized algorithm that can be applied to the path synthesis problems of the four-bar linkage and to analyze the optimization results. Seven test functions were used to verify the algorithm as a new method. The method was then used as a tool for the path synthesis problems of the four-bar linkage. Because two single methods are hybridized, it is expected that the proposed method will have some strengths and weakness. By analyzing the results compared to the other single and hybridized method, this study suggests the feasibility and limitations of the developed algorithm.

3.2. Taguchi method

The TM was developed by Dr. Genichi Taguchi as a methodology for the application of designed experiments [33]. This is an engineering methodology for optimizing the quality of a product, and process conditions that are sensitive to the causes of variation. The contribution of this method is that it makes a practitioner's work simpler by providing fewer experimental designs, and by providing a clearer understanding of the variational nature and economic consequences of quality engineering in the world of manufacturing [35, 36]. There are two major tools used in the TM: an orthogonal array, and the signal-to-noise-ratio (SNR).

Our proposed algorithm uses two-level or three-level orthogonal arrays. We briefly introduce the basic concept of the structure and use of three-level orthogonal arrays in this section. Additional details, and a detailed description of other levels of orthogonal arrays, can be found in the book presented by Peace [33]. Matrices called orthogonal arrays are widely used. In designed experiments, each column is orthogonal to other columns to determine which combinations of factor levels, which are representative of the actual values of design variables, to use for each experimental run, and for analyzing the data. It is a matrix of numbers arranged in rows and columns such that each row represents the level of the factors in each

experimental run, and each column represents a specific factor that can be changed from each experimental run.

The general symbol for a three-level standard orthogonal array is

$$L_n\left(3^{\frac{n-1}{2}}\right) \tag{7}$$

where

$n = 3^k$	is the number of experimental runs;
k	is a positive integer that is greater than 1;
3	is the number of levels for each factor; and
$\frac{(n-1)}{2}$	is the number of columns in the orthogonal array.

The three-level orthogonal arrays most often used in practice are $L_9(3^4)$, $L_{27}(3^{13})$ and $L_{81}(3^{40})$. Table 3 shows the orthogonal array $L_9(3^4)$, which is one of the basic orthogonal arrays. In a simple optimization algorithm such as exhaustive search, it takes $81(3^4)$ experiments to find optimal point, but the TM using an orthogonal array needs only nine experiments to find an optimal point (the details can be found in [33]). Because of this benefit, the TM is an effective optimization algorithm for finding optimal points.

The reason TM is an important tool for robust design is that TM uses the SNR. The SNR is the value that combines the mean of some quality characteristic and the variance of the characteristic. So, the meaning of maximizing the SNR value is to find the optimal value and to minimize the variance in the noise environment.

Table 3 $L_9(3^4)$ orthogonal array

Experiment Number	Factors			
	A	B	C	D
	Column number			
	1	2	3	4
1	1	1	1	1
2	1	2	2	2
3	1	3	3	3
4	2	1	2	3
5	2	2	3	1
6	2	3	1	2
7	3	1	3	2
8	3	2	1	3
9	3	3	2	1

However, because the function value used in this dissertation is not affected by the environment, the SNR is not necessary in this dissertation.

3.3. Random coordinate search algorithm

The details of RCA are summarized in Fig. 13. In addition to the basic algorithm, two other strategies to find global optimal point are used in this study. One is an additional optimal test. If a function value is not updated while all coordinates are modified, the point is suspected of being a local optimal point. Because of the random order, it is not clear if the point is a local optimum. It is possible that other optimal points exist when all coordinates are modified according to other random order set. Therefore, we add more optimal tests with random order to escape the local optimal points.

Problem :	$\min_{x \in R^n} f(x)$
	Where $f: R^n \to R \cup \{\infty\}$
Input:	$x_0 \in R^n$ // starting point
	$\alpha_0 > 0$ // initial step size
	Max step size
	Max test number // needs additional minimum test due to the random order generation
	$k = 0$ // index
	$t_{iter} = 1$ // test index
While(α_k <max step size)	
	Generate random order without duplication, $\mathrm{RO} = [2, 3, 4, \dots] \in R^n$
	Make the flag matrix, $\mathrm{F} = [1,1, \dots 1] \in R^n$
	for i=0,1,…n-1
	if $f(t) < f(x_{nk+i})$ for some $t \in P_{nk+i} := \{x_{nk+i} \pm \alpha_k e_j : j = RO(i+1)\}$
	set $x_{nk+i+1} = t$
	otherwise $F(i+1) = 0$
	endfor;
	if sum(*F*)=0
	if t_{iter}= max test number
	$\alpha_{k+1} = \alpha_k + \alpha_0$ & $t_{iter} = 1$ // increase step size and initialize test number
	otherwise $\alpha_{k+1} = \alpha_k$ & $t_{iter} = t_{iter} + 1$ // increase test number
	otherwise $\alpha_{k+1} = \alpha_0$ // keep the step size
	$k = k + 1$
endwhile	

Figure 13 Random coordinate search algorithm

If the point passes the additional optimal test, there is one more test to find the global optimal point, which involves increasing the step size. The basic RCA procedure finds the optimal point by reducing the maximum step size to the minimum step size. This makes it clear that the point is a local optimal but does not prove the point to be a global optimum. So, the RCA was used to find the optimal point by increasing the minimum step size to the maximum step size. If the point is updated while increasing the step size, the RCA searches from the updated point with the initial step size again. This method requires many function evaluations, but it is clear that it finds the global optimal point.

3.4. Hybrid Taguchi-random coordinate search algorithm (HTRCA)

The HTRCA combines TM and RCA. A second TM is inserted between each RCA. This makes the HTRCA a very useful way to find the global optimal point. The steps of the HTRCA approach are depicted in Fig. 14.

The HTRCA derives effectiveness from the difference in step size. In the case of RCA, a precise optimal point is found using a small step size. On the other hand, the rough optimal point is found using a large step size in TM. Therefore, we expect that HTRCA can find the precise optimal point effectively. HTRCA also features diversity of the search direction. In the case of RCA, the search direction is restricted to the basis vector, while that in TM is not. Thus, we expect that HTRCA can find the optimal point more robustly by varying the search direction.

There are four strategies to distinguish a global optimal point from a local optimal point, three of which were mentioned in Section 3.3 (random order of coordinates, additional minimum test, and increasing the step size). The fourth strategy is using a second TM application after RCA. In the case of RCA, only one coordinate is modified in one step. So, if two or more variables are related to each other, as with the Rosenbrock parabolic valley function in Section 3.5.1.1, it can be hard to find the optimal point using only RCA. However, by using TM to modify two or more variables based on the orthogonal array in one step, it is possible to find the optimal point.

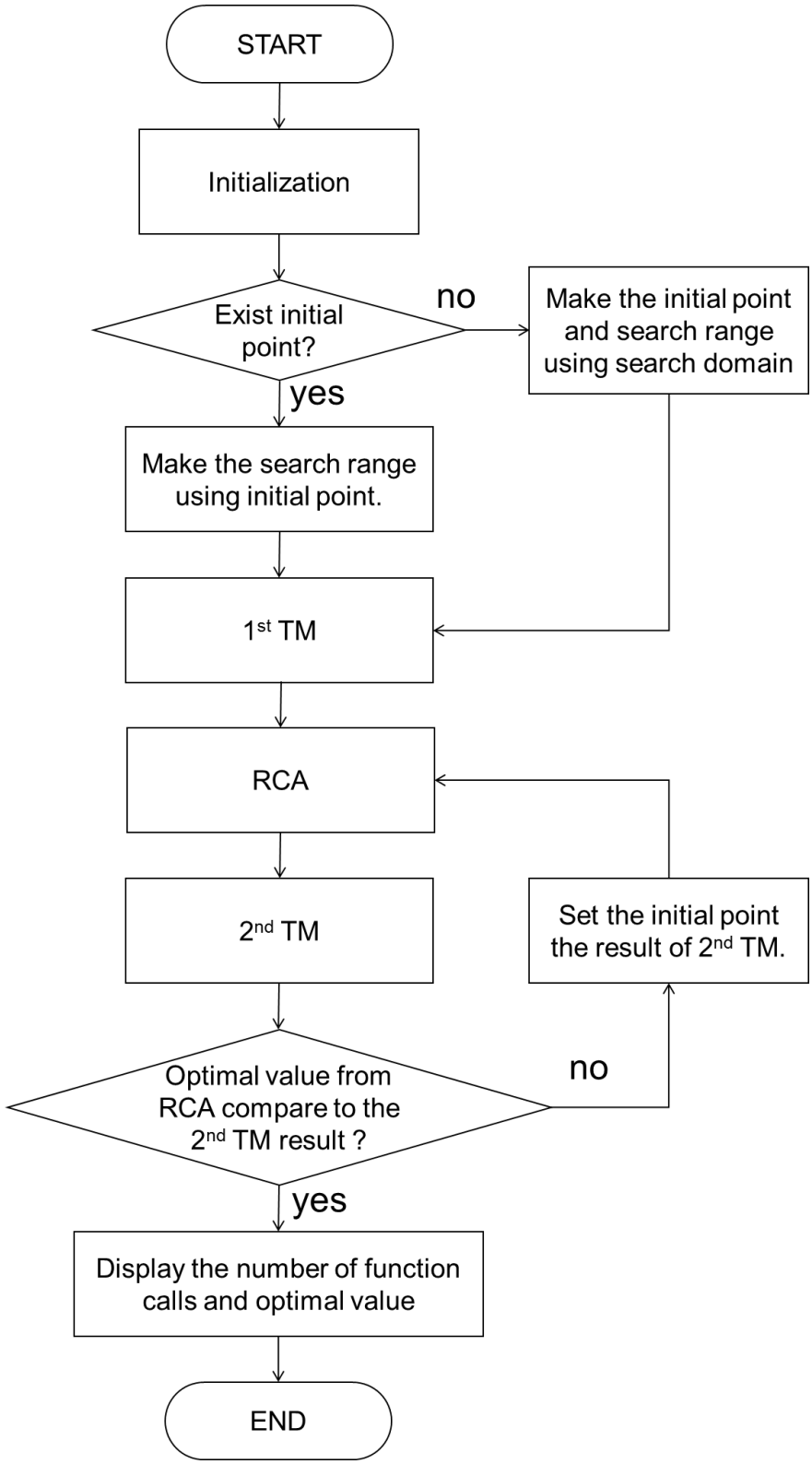

Figure 14 HTRCA for global optimization problem

3.5. Verification of HTRCA

3.5.1 Find the global optimum by test function analysis

3.5.1.1 Test functions

The proposed HTRCA is compared to RCA and the algorithm proposed by Li et al. [37], called random optimization algorithm hybridized with jumping-away algorithm. To compare the performances of each algorithm, seven benchmark functions found in the literature [38-40] are used. The functions are commonly used functions to test optimization performances of multidimensional continuous optimization problems. All the functions are to be minimized. These functions have multiple local minimum points in the pre-defined search domain. The number of local minima is also related to the complexity of the functions. The seven functions are defined as follows:

1. *Test function 1*

The six-hump camelback function [38, 39] is defined as follows:

$$f_1(x_1, x_2) = \left(4 - 2.1{x_1}^2 + \frac{{x_1}^4}{3}\right){x_1}^2 + x_1x_2 + (-4 + 4{x_2}^2){x_2}^2. \quad (7)$$

The function $f_2(x_1, x_2)$ has six local minima, two of which are global minima. The global minimum value is **-1.0316285**, and the search range is [-3 3].

2. *Test function 2*

The two-dimensional Shubert function [38, 39] is defined as follows:

$$f_2(x_1, x_2) = \left\{\sum_{i=1}^{5} i\cos\big((i+1)x_1 + i\big)\right\}\left\{\sum_{i=1}^{5} i\cos\big((i+1)x_2 + i\big)\right\} \quad (8)$$

The function $f_2(x_1, x_2)$ has 760 minima, one of which is the global minimum. The global minimum value is **-186.73091**, and the search range is [-5.12 5.12].

3. *Test function 3*

The third test function defined in [38, 39] are defined as follows:

$$f_3(X) = \frac{\pi}{5}\left\{10\sin^2(\pi x_1) + \sum_{i=1}^{4}[(x_i - 1)^2(1 + 10\sin^2(\pi x_{i+1}))] + (x_5 - 1)^2\right\} \quad (9)$$

where X={x_1, x_2, x_3, x_4, x_5}

The function has approximately 10^5 local minima and a unique global minimum. The global minimum value is **0**, and the search range is [-2 2].

4. *Test function 4*

The fourth test function [38, 39] is defined as follows:

$$f_4(X) = 0.1\left\{\sin^2(3\pi x_1) + \sum_{i=1}^{6}[(x_i - 1)^2(1 + \sin^2(3\pi x_{i+1}))] + (x_y - 1)^2(1 + \sin^2 2\pi x_7)\right\} \quad (10)$$

where X={x_1, x_2, x_3, x_4, x_5, x_6, x_7}

The function has roughly 157 local minima and unique global minimum. The global minimum value is **0**, and the search range is [-2 2].

5. *Test function 5*

The Rosenbrock parabolic valley function [40] is defined as follows:

$$f_5(x_1, x_2) = 100(x_2 - x_1^2)^2 + (1 - x_1)^2 \quad (11)$$

The function has a unique global minimum. The global minimum value is **0**, and the search range is [-4 4].

6. *Test function 6*

The Powell quartic function [40] is defined as follows:

$$f_6(X) = (x_1 + 10x_2)^2 + 5(x_3 - x_4)^2 + (x_2 - 2x_3)^4 + 10(x_1 - x_4)^4 \quad (12)$$

where X={x_1, x_2, x_3, x_4}

The function has unique global minimum. The global minimum value is **0**, and the search range is [-4 5].

7. *Test function 7*

The Fletcher and Powell helical valley function [40] is defined as follows:

$$f_7(x_1, x_2, x_3) = 100[x_3 - 10\theta(x_1, x_2)]^2 + \left[\sqrt{x_1^2 + x_2^2} - 1\right]^2 + x_3^2 \qquad (13)$$

where $2\pi\theta(x_1, x_2) = arctan(x_2/x_1)$ for $x_1 > 0$, and $\pi + arctan(x_2/x_1)$ for $x_1 < 0$. The function has unique global minimum. The global minimum value is **0**, and the search range is [-2 2].

3.5.1.2 Results and comparison

To compare the performances of optimization algorithms, cost function is defined as follows:

$$f_{cost}(X) = (f_0(X_0) - f(X))^2 \qquad (14)$$

where $f(X_0)$ is the known global minimum at X_0, and $f(X)$ is the determined optimal. The acceptable cost is set to be 1×10^{-4}.

The numerical results averaged over 25 trials for each test functions are shown in Tables 4–6. The results show that the proposed HTRCA is much better in success rate than RCA and in function evaluation than Li et al. [37]. The proposed HTRCA has the ability of finding the global minima with 100% success rate as shown in Table 4, while the RCA with same setting only shows 62.9%(110/175) success rate. From the results shown in Tables 4 and 5, we can see that 2nd TM in RCA contributes significantly to success ratio to find global minimal values of the seven test functions. The 2nd TM in HTRCA works to avoid being trapped in local minima.

Table 4 Numerical results of average 25 trials (the proposed HTRCA).

	Successes of 25 trials	Aveg. Function evaluations	Accuracy	2nd TM
Test function 1	25	223.0	1.98E-07	2.00
Test function 2	25	785.6	6.00E-06	7.16
Test function 3	25	466.2	6.69E-58	2.00
Test function 4	25	551.1	4.05E-59	2.00
Test function 5	25	74,560	2.69E-05	129
Test function 6	25	2150	1.10E-05	2.00
Test function 7	25	26,670	3.29E-05	24.2

Table 5 Numerical results of average 25 trials (the RCA)

	Successes of 25 trials	Aveg. Function evaluations	Accuracy
Test function 1	22	181.8	1.98E-07
Test function 2	6	470.0	6.28E-06
Test function 3	25	348.0	4.27E-58
Test function 4	25	432.1	6.97E-59
Test function 5	3	3407	1.45E-05
Test function 6	22	2748	1.55E-05
Test function 7	7	2401	2.60E-05

Table 6 Numerical results of average 25 trials (the algorithm in Reference [37])

	Successes of 25 trials	Aveg. Function evaluations	Accuracy
Test function 1	25	629.5	3.14E-05
Test function 2	25	2715	1.60E-05
Test function 3	25	1351	5.63E-05
Test function 4	25	4091	6.72E-05
Test function 5	25	618.4	2.50E-05
Test function 6	25	3271	4.23E-05
Test function 7	25	7089	3.84E-05

The proposed HTRCA is also compared to the algorithm given in Reference [37]. The algorithm in Reference [37] shows perfect success rate as the proposed HTRCA. It is important to compare the function evaluations and accuracy of each algorithm shown in Tables 4 and 6. In the most of the test functions except test function 5 (Rosenbrock parabolic valley function) and function 7 (Fletcher and Powell helical valley function), the function evaluations of HTRCA are smaller than the function evaluation of the algorithm in Reference [37]. Also, in all test functions, HTRCA finds optimal value more accuracy despite function evaluations are less than that of the algorithm in Reference [37].

3.5.2 Path synthesis of four-bar linkage

The HTRCA has been verified as robust optimization algorithm through the seven test functions in the previous section. In this section, performance of the optimization algorithm as a good tool for path synthesis will be tested.

3.5.2.1 Case study 1: liner motion generation without prescribed timing

The first problems chosen here is from a study done by Cabrera et al. [19]. The desired trajectory is composed of six points to find out an optimal solution, which is a vertical straight line. Thus, this problem is described as follows:

Desired points:

$C_d^i = [(20, 20), (20, 25), (20, 30), (20, 35), (20, 40), (20, 45)]$

Constraint of the variables:

$l_1, l_2, l_3, l_4, \in [5, 60]$;

$l_{cx}, l_{cy}, x_0, y_0, \in [-60, 60]$;

$\theta_0 \in [0,2\pi]$

3.5.2.2 Case study 2: path generation with prescribed timing

The second case study is a problem of path generation with prescribed timing [28]. The desired trajectory, which is a semi-circular arc, is composed of six points. This problem:

Desired points:

$C_d^i =$

$[(0, 0), (1.9098, 5.8779), (6.9098, 9.5106), (13.09, 9.5106), (18.09, 5.8779), (20, 0)]$

Constraint of the variables:

$\theta_d^i = \left[\frac{\pi}{6}, \frac{\pi}{3}, \frac{\pi}{2}, \frac{2\pi}{3}, \frac{5\pi}{6}, \pi\right]$

$l_1, l_2, l_3, l_4, \in [5, 50]$;

$l_{cx}, l_{cy}, x_0, y_0, \in [-50, 50]$;

$\theta_0 \in [0,2\pi]$

3.5.2.3 Case study 3: path generation without prescribed timing

The final case is a problem of path generation with prescribed timing [28]. The desired trajectory, which is an elliptical path, is composed of ten points. This problem:

Desired points:

$$C_d^i =$$

$$[(20,10),(17.66,15.142),(11.736,17.878),(5,16.928),(0.60307,12.736),$$
$$(0.60307,7.2638),(5,3.0718),(11.736,2.1215),(17.66,4.8577),(20,10)]$$

Constraint of the variables:

$l_1, l_2, l_3, l_4, \in [5,80]$;

$l_{cx}, l_{cy}, x_0, y_0, \in [-80,80]$;

$\theta_0 \in [0,2\pi]$

3.5.2.4 Optimization and results

To Figure out the optimal solution, we set the parameter of the HTRCA as follows;

Table 7 Parameter setting of the HTRCA in path synthesis

Parameter setting of Taguchi method			
Step size of 1st TM	: 1/5 of search range	Orthogonal array	:$L_{27}(3^{13})$
Step size of 2nd TM	: 1/100		
Parameter setting of RCA			
Initial step size	: 1/500	Max test number	: 100
Max step size	: 1/5		

The results of case 1 are tabulated in Table 8 and Fig. 15 with the results obtained by [7,27 and 28]. The optimal value of the objective function (=T.E.) using proposed HTRCA is the second minimum value among the results. In case of case study 2, the results are tabulated in Table 9 and Fig. 16. The optimal value of the objective function is 3.571 which is comparable to the result of the other evolutionary algorithm from [7,28]. The results of last case are tabulated in Table 10 and Fig. 17.

Table 8 Comparative results for case 1.

	Cabrera et al.[27]	GA[28]	PSO[28]	DE[28]	GA–DE [7]	HTRCA
l_4	39.46629	28.77133	31.15501	35.02074	33.5959	18.42
l_1	8.562912	5	5	6.404196	5.02972	35.14
l_2	19.09486	35.36548	23.84561	31.60722	11.1847	56.42
l_3	47.83886	59.13681	45.80352	50.59949	28.0878	49.99
l_{cx}	13.38556	0	39.00066	20.80324	-24.1755	55.08
l_{cy}	12.21961	14.85037	18.50846	41.54364	5.51479	-59.52
x_0	29.7225	29.91329	59.99999	60	39.7799	-25.92
y_0	23.4545	32.60228	17.91696	18.07791	24.7195	42.12
θ_0	6.20163	5.287474	0.419837	0	5.45884	5.9313
θ_1^1	6.11937	6.283185	4.842412	6.283185	6.80719	2.347398
θ_1^2	0.19304	0.318205	0.404684	0.264935	0.853145	2.584902
θ_1^3	0.44083	0.63852	0.657415	0.500377	1.16505	2.84754
θ_1^4	0.68467	0.97995	0.922086	0.735321	1.49253	3.117717
θ_1^5	0.95835	1.412732	1.247066	0.996529	1.87456	3.376584
θ_1^6	1.35533	2.076254	2.298727	1.333549	2.44206	3.611575
f_{obj}(=T.E.)	0.19047	1.101697	0.546461	0.122738	0.0007369	0.0056

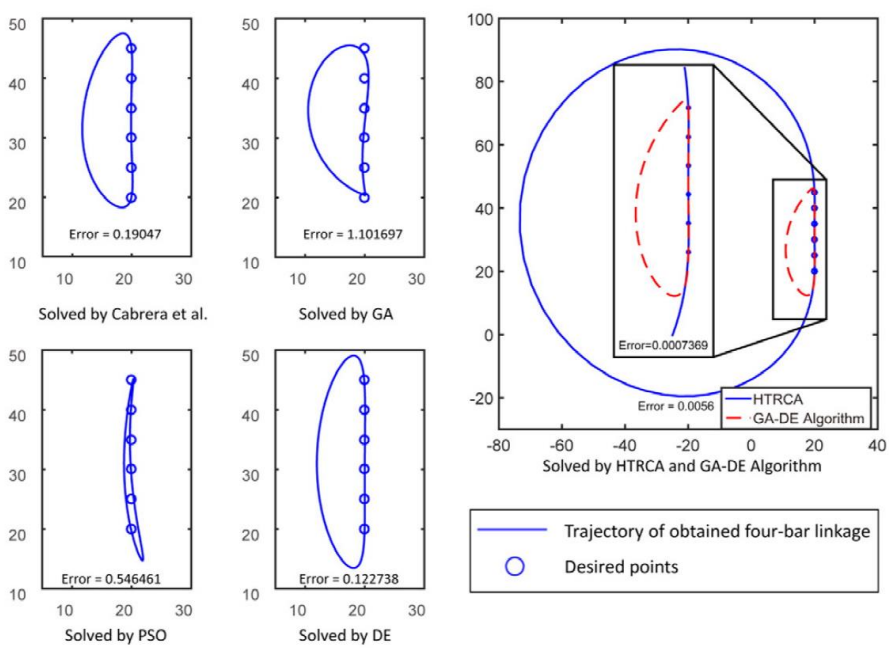

Figure 15 Coupler curves obtained in Case 1

Table 9 Comparative results for case 2.

	GA[28]	PSO[28]	DE[28]	GA–DE [7]	HTRCA
l_4	50	49.99486	50	50	49.46
l_1	9.164414	5	5	5	5.405
l_2	16.85808	5.915643	5.905345	6.97009	8.015
l_3	50	49.99487	50	48.1993	47.165
l_{cx}	38.45887	18.92572	18.81931	17.045	17.9
l_{cy}	0.090117	0	0	12.638	15.3
x_0	32.32828	14.47248	14.37377	12.2377	12
y_0	-29.53705	-12.4944	-12.4443	-15.8332	-18.7
θ_0	0.877212	0.467287	0.463633	0.0508453	6.2832
f_{obj}(=T.E.)	3.171063	2.35529	2.349649	2.58286	3.571

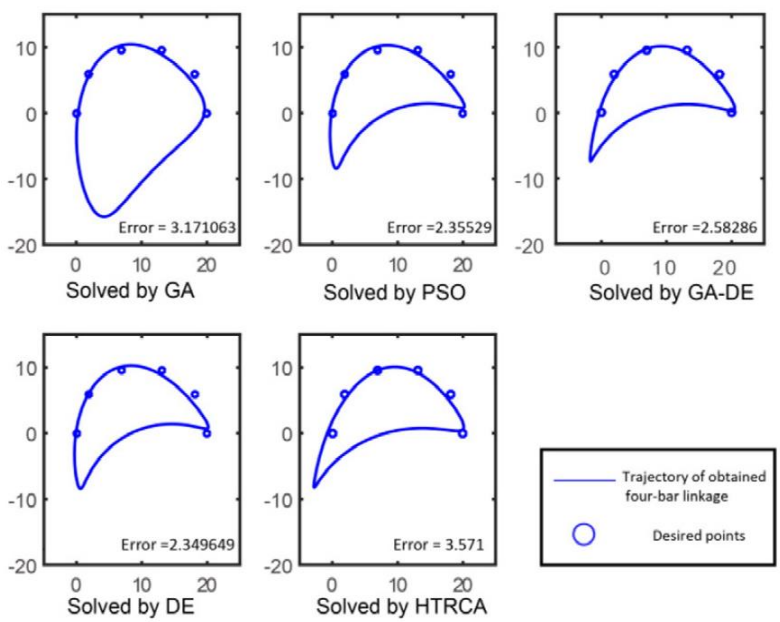

Figure 16 Coupler curves obtained in Case 2

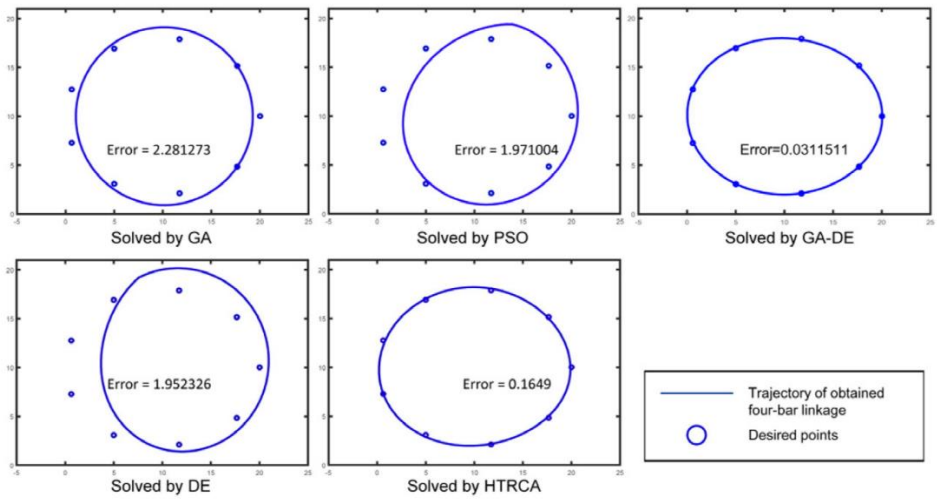

Figure 17 Coupler curves obtained in Case 3

Table 10 Comparative results for case 3.

	GA[28]	PSO[28]	DE[28]	GA–DE [7]	HTRCA
l_4	79.98151	52.53516	54.36089	80	54.875
l_1	9.109993	8.687886	8.683351	8.24689	9.725
l_2	72.93651	36.15508	34.31863	45.8968	49.925
l_3	80	80	79.99617	58.5404	23.375
l_{cx}	0	0	0.000187	- 6.40389	7.84
l_{cy}	0	1.481055	1.46525	- 9.12264	-4.32
x_0	10.15597	11.00212	10.9544	6.52409	1.44
y_0	10	11.09559	11.07453	20.522	12.16
θ_0	0.026149	1.403504	2.12965	0.136532	6.1135
θ_1^1	6.283185	6.282619	6.283185	6.05991	0.148283
θ_1^2	0.600745	0.615302	0.616731	0.488453	0.825611
θ_1^3	1.372812	1.305421	1.310254	1.17805	1.520531
θ_1^4	2.210575	2.188053	2.19357	1.88339	2.236814
θ_1^5	2.862639	2.913049	2.91717	2.59806	2.906602
θ_1^6	3.420547	3.499313	3.490746	3.28585	3.565079
θ_1^7	4.072611	4.125586	4.132017	3.96674	4.295185
θ_1^8	4.910373	4.919977	4.922075	4.65966	5.021522
θ_1^9	5.68244	5.685021	5.695372	5.35231	5.718955
θ_1^{10}	6.283185	6.282323	6.28297	6.06263	0.148283
f_{obj}(=T.E.)	2.281273	1.971004	1.952326	0.0311511	0.1649

3.5.3 Discussion

As mentioned in the previous sections, the HTRCA is a hybrid algorithm combining RCA and TM. The TM is used to determine the initial point and also TM is inserted between each run of the RCA. The combination of two algorithms shows improved characteristics from the comparison results.

Firstly, robustness is improved. HTRCA can find optimal value in all test functions while the RCA cannot find the optimal value in some functions (Test function 1, 2, 5, 6 and 7). It means that TM inserted between each run of the RCA work to escape local minima successfully. Secondly, effectiveness is improved. HTRCA can find optimal value using less function evaluations than algorithms in Reference [37] which is random optimization algorithm including a jumping-away mechanism (except test function 5 and 7). Also, HTRCA can find optimal value more accurate than the algorithm of Reference [37]. Therefore, HTRCA can be considered to be more effective than the algorithm in Reference [37].

To find the optimal point of test functions 5 and 7, the HTRCA calls too many TM during the RCA loop. We believe that is the reason of high function evaluation to find the global optimal. Reducing the number of calling 2nd TM is remained as a future work to increase the effectiveness of the HTRCA.

Proven HTRCA is used as a tool for path synthesis of four-bar linkage in Section 3.5.2. The result show that the HTRCA can find the comparative results. In details, HTRCA obtain the best solution among the single evolutionary algorithm form [28] in case study 1 and 3. However, compared to the hybrid algorithm GA–DE [7], the HTRCA cannot find the better solution. Nevertheless, the difference between the results from HTRCA and the GA–DE is thought to be negligible. In case 2, the result of HTRCA is the worst solution among the other algorithm from [7,28]. The T.E. values of each method (2.3 ~ 3.5) in this case are larger than that of the other method (0.0007 ~ 2.3). This implies that the optimal solution which can trace the target points well is not existing. In this situation, hybrid algorithms (HTRAC and GA–DE) cannot obtain the optimal solution compared to the single optimization algorithm such as PSO and DE. However, we thought that the difference between hybrid algorithms and the other method is reasonable.

3.6. Conclusion

We propose a hybrid global optimization algorithm based on the Taguchi method and the random coordinate search algorithm for path synthesis of four-bar linkage. From the first optimal point generated by TM using the randomly generated initial point, RCA is performed to change one coordinate with random order at one step. Then, using a second application of the TM, HTRCA tests whether the point is a local optimal or not. The HTRCA is a very robust and effective way to find an optimal point. Seven test functions were used to verify the robustness and effectiveness of the HTRCA algorithm. By inserting TM between each RCA, the success ratios were improved for complex test functions. Also, HTRCA can minimize test functions more effective than other optimization algorithm in not only function evaluation, but also accuracy. There is a limitation of the HTRCA in that some tests require many function evaluations.

In addition, we present a tool for path synthesis of four-bar linkage. Despite, HTRCA cannot achieve the best optimal solution in overall cases, the method can find the reasonable optimal solutions compared to the other single evolutionary algorithms and hybrid algorithm such as genetic algorithm, particle swarm optimization, differential evolution and GA−DE hybrid algorithm. Therefore, we saw the possibility to adopt the developed algorithm to a tool for path synthesis of four-bar linkage.

Chapter 4 Verification and applications

This chapter analyzes a number of cases that were investigated with the developed algorithm to validate the design methodology. For a performance comparison, the conventional method that minimizes tracking error is used. The input data set of the given points and their intervals is controlled for unprejudiced comparison. The performance index called 'Goodness of Traceability' is defined to compare the results from each method.

4.1. Case studies

4.1.1 Case 1–1: type-I (equal intervals)

The desired trajectory of the first case is a mathematical ellipse described as follows:

$$\frac{(x-x_0)^2}{a^2}+\frac{(y-y_0)^2}{b^2}=1 \tag{14}$$

1,000 coupler points were chosen to identify the optimal solution that can trace an ellipse with a=100 and b=50. Because the purpose of this case study is to find the shape and size of the trajectory, the position variables x_0 and y_0 are not needed. Therefore, for this problem,

Target curve:

$C_{x,D} = 100\cos\theta$

$C_{y,D} = 50\sin\theta$

$\theta = i/1000\,, i = 1, \ldots, 1000$

Constraint conditions:

Desired shape: Type-I

$X_{size} \in (\ 0, 500\ ]$

$[l_2 \quad l_3 \quad l_4]/l_1 \in (\ 0, 10\ ]$

$[l_{cx} \quad l_{cy}]/l_1 \in [\ -10\ , 10]$

4.1.2 Case 1–2: type-I (variable intervals)

This case is also an ellipse described by equation (14). In some real situations, the velocity of each section needs to be considered. Therefore, the velocity profile of the coupler points is modified from the first case. The other conditions are the same. For this problem,

Target curve:

$$C_{x,D} = \begin{cases} 100\cos\left(\frac{i}{550}\pi\right) & i = 1,\dots,550 \\ 100\cos\left(\pi + \frac{i-550}{450}\pi\right) & i = 551,\dots,1000 \end{cases}$$

$$C_{y,D} = \begin{cases} 50\sin\left(\frac{i}{550}\pi\right) & i = 1,\dots,550 \\ 50\sin\left(\pi + \frac{i-550}{450}\pi\right) & i = 551,\dots,1000 \end{cases}$$

Constraint conditions:

Desired shape: Type-I

$X_{size} \in (\ 0, 500\ ]$

$[l_2 \quad l_3 \quad l_4]/l_1 \in (\ 0, 10\ ]$

$[l_{cx} \quad l_{cy}]/l_1 \in [\ -10\ , 10]$

4.1.3 Case 2–1: type-III (equal intervals)

The desired trajectory of case 2 looks like a crescent, as shown in Fig. 15 (a). The desired velocity in all sectors is constant. For this problem, the target curve and constraint conditions are as follows.

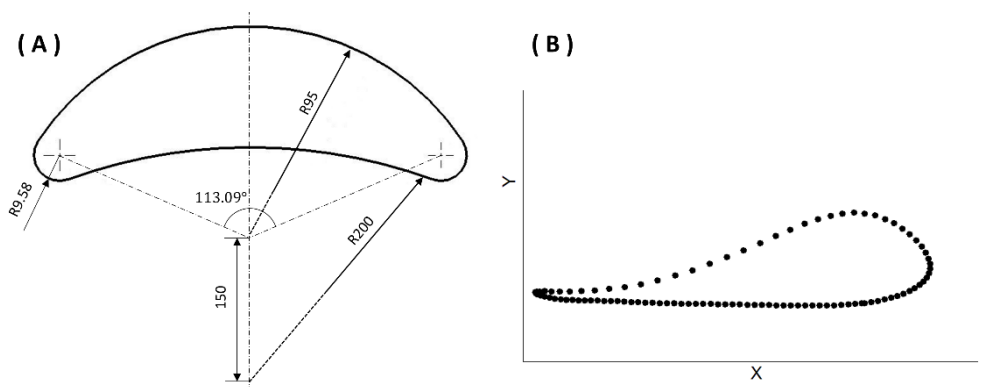

Figure 18 Desired trajectories of case study (A) Case 2 (B) Case 3

Target curve:

The value of parameter composing the shape of the desired trajectory is demonstrated in Fig. 15 (a).

1,000 coupler points in total are positioned equidistantly.

Constraint conditions:

Desired shape: Type-III

$X_{size} \in (\ 0, 100\ ]$

$[l_2 \quad l_3 \quad l_4]/l_1 \in (\ 0, 10\ ]$

$[l_{cx} \quad l_{cy}]/l_1 \in [\ -10\ , 10]$

The distance between centerline and input point is smaller than 20.

4.1.4 Case 2–2: type-III (variable intervals)

The shape of the trajectory in this case is the same as case 2–1, except for the desired velocity of each section. Instead of constant velocity, the velocity of the lower side of the trajectory is 10% slower than that of the previous case with the same constraints. Therefore, for this problem, the target curve and constraint conditions are as follows.

Target curve:

The shape of the trajectory is the same as case 2–1

The interval between each points of the upper side is 10% larger than that of case 2–1.

The interval between each point of the lower side is 10% smaller than that of case 2–1.

4.1.5 Case 3: Avoiding intersectional shapes

This case is from a real application of generating a human gait trajectory for the rehabilitation of a person who has difficulties in walking. The human gait trajectory was captured by a motion capture system, and 101 coupler points were composed, as illustrated in Fig. 15 (b). For this problem, the target curve and constraint conditions are as follows.

Target curve:

The trajectory shape is depicted in Fig. 15 (b).

101 points captured by motion capture system.

Constraint conditions:

Desired shape: Type-I, II, and III

$X_{size} \in (\ 0, 200\ ]$

$[l_2 \quad l_3 \quad l_4]/l_1 \in (\ 0, 10\ ]$

$[l_{cx} \quad l_{cy}]/l_1 \in [\ -10\ , 10]$

4.2. Comparative results and discussion

4.2.1 Goodness of traceability(GT) index for objective comparison

To compare the performance of each method, an index for objective comparison is necessary. If the value of the developed objective function is used for comparing the performance, the new method minimizes that value and will naturally show better performance than other methods. There are various indexes that evaluate the performance of a design methodology. The most common index is tracking error, as mentioned. Because only the distance between the generated trajectory and target is calculated, TE cannot represent the velocity of the coupler point. Other indexes such as mismatch area error [41] and structure error [42] also cannot represent the velocity of the coupler point. Therefore, we defined the GT index, which can represent the shape and velocity simultaneously for objective comparison. GT is defined as the tracking error according to the input angle(=time).

4.2.2 The result and discussion

The case study results are shown in Table 11. Fig. 19 shows the obtained trajectory and the position of the coupler point according to the input angle of case 1-1 and case 1-2. The trajectory shapes obtained by the TE-minimizing method are the same in cases 1-1 and 1-2. In contrast, the shapes obtained by the new method are different for these cases. These results show that the proposed approach can take account of the velocity profile of each section of the trajectory, in contrast to the conventional TE approach. There are two peaks in the reference. If the results do not follow these peaks, RMSEs of first and second order derivative are very large. Thus, to minimize the objective function, the peaks of slope and the change in angle of slope of the generated mechanism have to match with the reference naturally. It

implies that the time portion of each section (upper and lower) of the generated mechanism is the same as that of the reference. This is the reason that the new method

Table 11 Comparative results of case 1

	Case 1-1		Case 1-2	
	Propsed	TE	Propsed	TE
l_1	68.37	50.50	81.12	50.50
l_2	417.03	157.81	494.84	157.81
l_3	403.35	282.80	527.28	282.80
l_4	676.81	361.08	766.59	361.08
l_{cx}	88.88	-118.68	811.21	-118.68
l_{cy}	-252.95	-90	381.26	-90
θ_0	-0.3253	3.2987	2.6755	3.2987
GT	2.0896	3.5437	2.7146	6.8365

Table 12 Comparative results of case 2 and 3

	Case 2-1		Case 2-2		Case 3	
	Propsed	TE	Propsed	TE	Propsed	TE
l_1	13.6	22.13	14.5016	22.13	184.00	193.60
l_2	29.24	48.12	24.64754	48.12	336.60	344.80
l_3	76.84	206.87	40.59855	206.87	346.60	378.20
l_4	89.76	219.59	50.02718	219.59	464.27	509.27
l_{cx}	136	212.40	-92.7999	212.40	404.41	382.21
l_{cy}	-102	65.2687	-18.8499	65.2687	155.08	205.88
θ_0	0.0135	3.2515	0.4749	3.2515	2.5483	2.4428
GT	7.2603	7.8451	7.5514	7.5989	46.3896	51.4451

can take account of the velocity of each section of the trajectory.

The GT values show this advantage very well. The GT values of the proposed method are smaller than those of the conventional method in both cases 1-1 and 1-2. This indicates that the new method can take account of the trajectory shape and velocity simultaneously.

The results of case 2 are shown in Fig. 20. Considering only the trajectory shape, the performance of the new approach is poorer than that of the conventional method.

However, the GT of the new approach is lower than that of the method that minimizes TE. Despite the conventional trajectory looking similar to the desired trajectory, the error of the x value according to the input angle is larger than that of the result from the new method, as shown on the right side of Fig. 20. This result also shows the velocity consideration of the new approach.

The results of case study 3 are depicted in Fig. 21. The intersectional shape of the trajectory is obtained by the TE-minimizing method. The purpose of this problem is a rehabilitation application. With the conventional method, a four-bar linkage that makes an intersectional trajectory shape cannot be the solution. The trajectory shape obtained by the new approach does not have an intersectional point, which satisfies the requirements, as shown in Fig. 21. The GT of the new approach is also smaller than that of the conventional method. The four bar linkage mechanisms from the result of case studies are demonstrated in Figs. 22, 23 and 24.

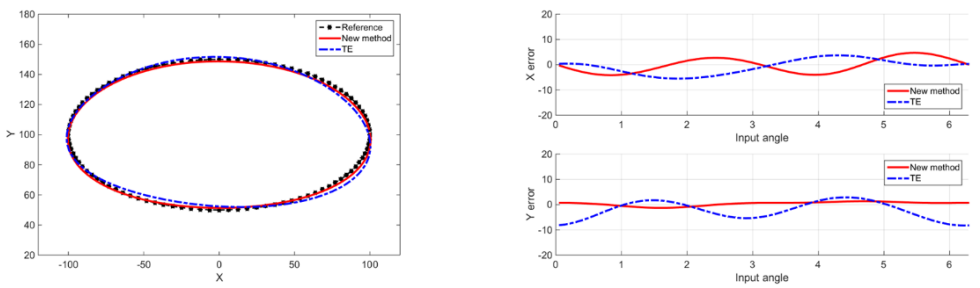

< Simulation Result of Case 1-1 (Left) Trajectory of coupler point (Right upper) X error V.S. input angle (Right lower) Y error V.S. input angle >

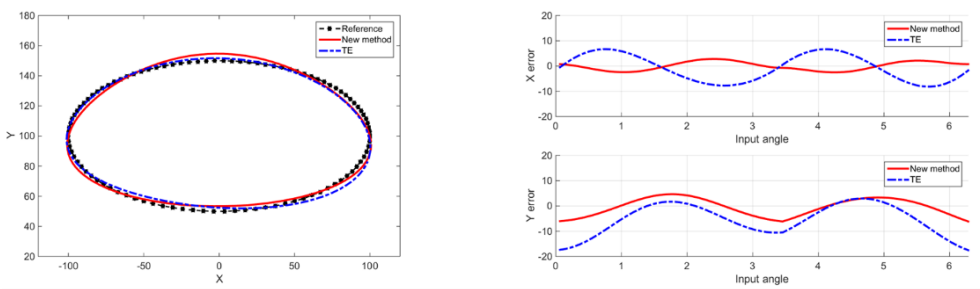

< Simulation Result of Case 1-2 (Left) Trajectory of coupler point (Right upper) X error V.S. input angle (Right lower) Y error V.S. input angle >

Figure 19 Simulation result of case 1 (ellipse shape)

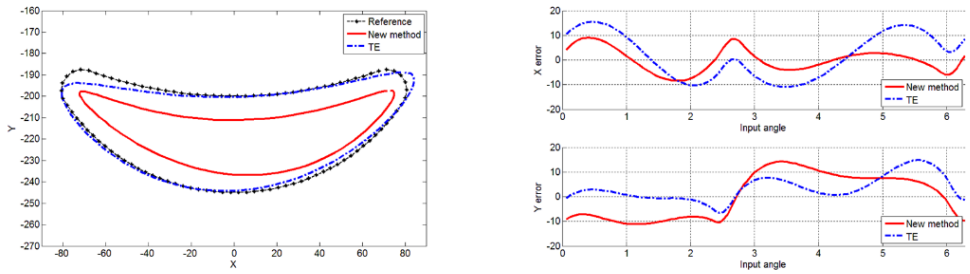

< Simulation Result of Case 2-1 (Left) Trajectory of coupler point (Right upper) X error V.S. input angle (Right lower) Y error V.S. input angle >

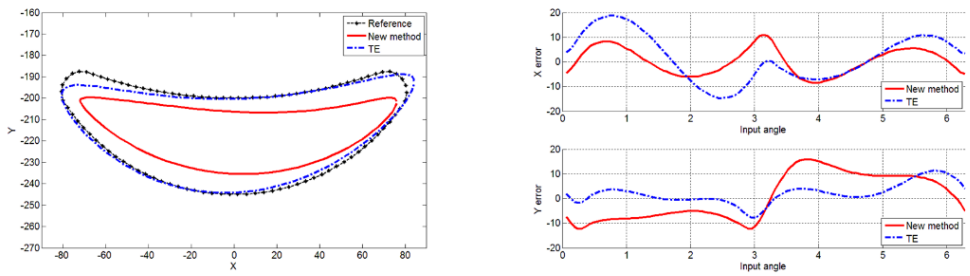

< Simulation Result of Case 2-2 (Left) Trajectory of coupler point (Right upper) X error V.S. input angle (Right lower) Y error V.S. input angle >

Figure 20 Simulation result of case 2 (crescent-like shape)

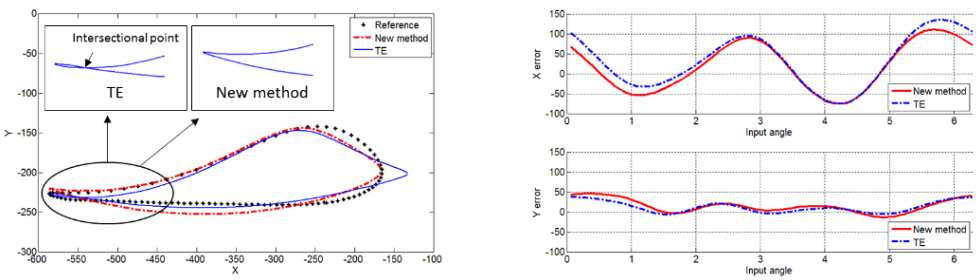

Figure 21 Simulation result of case 3 (walking motion)

The proposed design method is more reliable than the TE-based method, because there is no possibility of generating unintended shapes. In addition, the method includes the velocity profile, which allows the design method to obtain trajectories with various velocities.

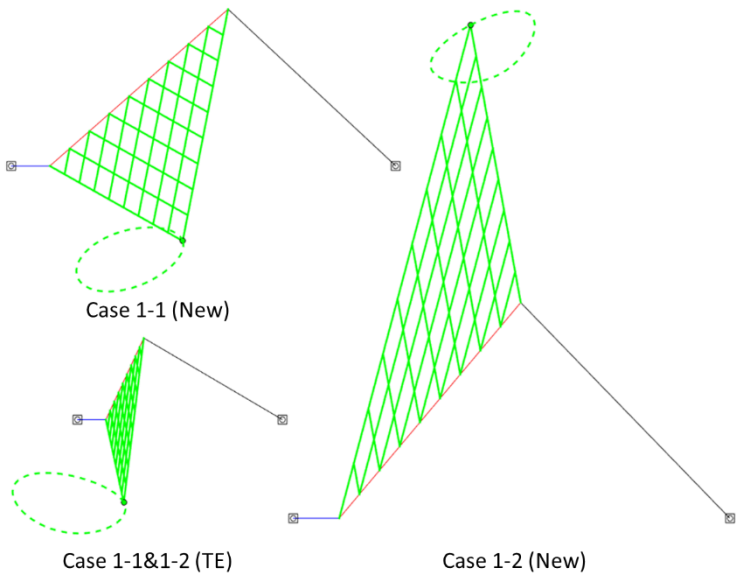

Figure 22 Four-bar linkage mechanism of case study 1(Input link: blue link)

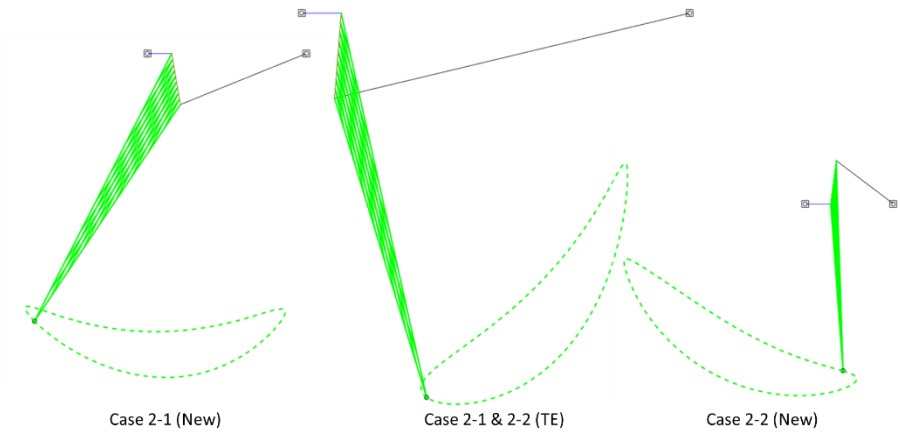

Figure 23 Four-bar linkage mechanism of case study 2(Input link: blue link)

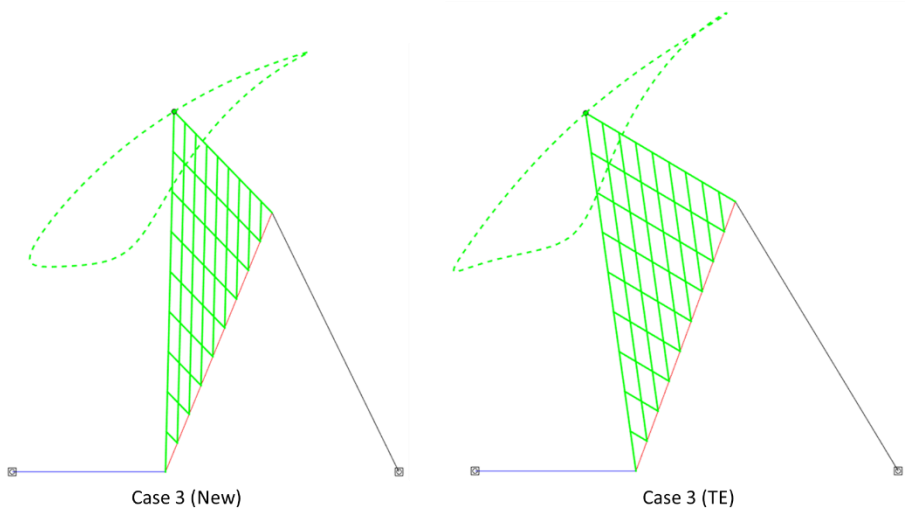

Figure 24 Four-bar linkage mechanism of case study 3(Input link: blue link)

4.3. Conclusion

In this chapter, the verifications of the proposed design methodology were conducted. The simulation results showed that the GT, which is used for the objective comparison, of the proposed path synthesis are the smaller than that of the conventional method in all cases. Therefore, I concluded that the method developed in this dissertation can be used for various design problem that figuring out the proper four-bar linkage.

Chapter 5 Conclusion

The trajectories of a crank-rocker four-bar linkage were grouped into four types, and a new methodology was presented based on the classification. The approach involved one step for minimizing the RMSE of the first-order derivative to obtain a similar trajectory shape and velocity to the target trajectory, and a second step to obtain an optimal size that can trace the target trajectory by minimizing the RMSE of the second-order derivative.

The proposed method has three advantages over the conventional method: the reference can be set to a continuous function, the method can take account of the velocity of each side of the trajectory, and it can avoid obtaining unintended trajectories based on the geometrical features. To compare the performance of the new approach objectively, the GT index was defined to take account of the shape and velocity of the trajectory simultaneously. The GT values showed the advantages of the new approach in case studies.

However, this methodology has some limitations. First, the target mechanism was limited to a crank-rocker four-bar linkage. Second, further work is needed to apply this new method to non-continuous target trajectories, such as in case 3. Future studies will be conducted to overcome these limitations. The practical applications will be examined in the part 2.

Part 2

Practical application

A new design of rotational transmission mechanism with dual four-bar linkages for non-servo motor type automatic tool changer

Chapter 1 Introduction

Due to the growth of demands of the efficient tapping center, the need of the non-servo motor type automatic tool changer(ATC), which is one of the components that enhance the efficiency of a tapping center, is also increased. Non-servo motor type ATC rotates the turret (the component of the ATC to load lots of tools) using the rotational power of main spindle transferred by the bevel gear. Because of the key way of the tool holder, the rotation of main spindle is restricted by multiples of 180 degrees. Therefore, the rotational transmission mechanism(RTM), which can convert the 180 degrees of rotation into specific angle of rotation (1/14 rotation), is required. In this dissertation, the new RTM with dual four-bar linkage is presented.

Some studies about non-servo motor type ATC have been conducted recently. The japan company Fanuc Ltd., developed the rotational transmission mechanism using three disks and many steel balls [47]. This mechanism has difficulty of manufacture and maintenance issue due to the heavy frictional force. Some company are try to use the planetary gear mechanism as a RTM. However, because of the heavy weight and manufacturing cost, it has not been commercialized.

In this dissertation, a new RTM for the non-servo motor ATC is presented. The RTM is based on dual four-bar linkage structure. The mechanism is composed of two four-bar linkages and one output plate. The mechanism is an intermittent RTM where a spoke in the four-bar linkage transfers rotating motion to the output plate by transferring the force through a pre-defined path. When a four-bar linkage drives the output plate, only 50% of the trajectory made by the coupler point of the four-bar linkage is used, resulting in intermittent rotary motion. To make this intermittent rotary motion to continuous motion, two four-bar linkage are used to rotate the output plate alternatively. When one four-bar linkage loses contact with the output plate, the other four-bar linkage starts to contact the output plate. This mechanism is totally different from the mechanism using single four-bar linkage which is similar to the dijksman's mechanism [48]. In case of the single four-bar linkage mechanism, the shape of the trajectory is the only thing to be considered. However, in case of dual four-bar linkage, both the shape and the speed ratio of the contact and non-contact paths of the trajectory are considered. To do this, the design methodology developed

in the part 1 of this dissertation is used.

This mechanism has some advantages compared to other mechanisms. Because the mechanism is composed of some links and a plate, its structure is simple for transmitting rotational motion. This makes it easy to manufacture and reduces the cost compared to other mechanisms. The mechanism also has an advantage of space efficiency. Because the four-bar linkages are positioned on the output plate, the width of the mechanism is the same as the radius of the output plate. The space efficiency is better than that of other mechanisms such as gears, Geneva drives, and planetary gear mechanisms.

Chapter 2 Mechanism synthesis

2.1 Design concept

We started the design of the new RTM with the question of whether two four-bar linkages could drive continuously the rotation of a disk. There are similar RTM was found in a paper and a book written by dijksman [48] and Erdman & Sandor [49]. However, both of them were used single four-bar linkage. This implies that the motion of the output is intermittent which is similar to the output motion of Geneva drive. The concept design of RTM is demonstrated in Fig. 25.

The coupler points of two four-bar linkages, positioned on the output plate, make a crescent-like trajectory that rotates the output plate using the slit of the plate. When one coupler point starts contact with output plate, the other coupler point loses contact with output plate like (1) and (3) of Fig. 25. In this way, using two four-bar linkage, it is possible to rotate the output plate continuously. There are two design problems in making this design concept possible. The first one is figuring out a proper four-bar linkage. As mentioned before, when one four-bar linkage loses contact with the output plate, the other four-bar linkage start contact with the output plate. To figuring out such four-bar linkage, not only trajectory of coupler point of four-bar linkage, but also the velocity of the coupler point has to be considered. Therefore, in this part a new design method developed in the part 1 of this dissertation that can consider the shape and velocity profile of the trajectory simultaneously was used. The second problem is designing the output plate to make a specific rotational transmission ratio using kinematic analysis.

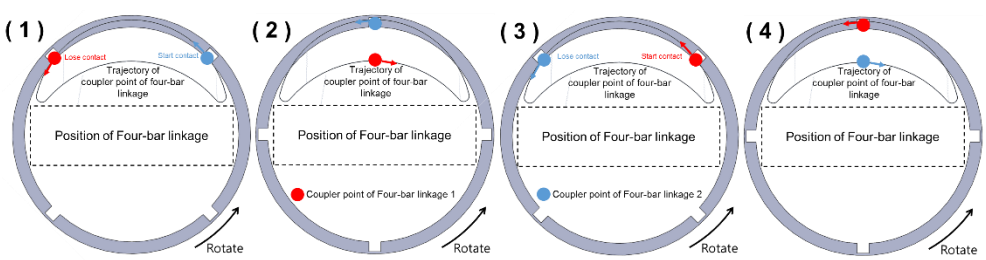

Figure 25 Design concept of the new rotational transmission mechanism

2.2 Four-bar linkage synthesis

2.2.1 Design objective

The design objectives of the mechanism synthesis are described as follows:

1. For continuous motion of the output plate, its duty factor is set to 1, the same as a gear mechanism.
2. The desired trajectory of the coupler point of the four-bar linkage is the crescent-like shape illustrated in Fig. 26
3. The part that drives the output plate is 50% of the entire trajectory of the four-bar linkage (Red part of Fig. 26).
4. Two four-bar linkages are used to drive the output plate alternately to make the duty factor of the output plate 1.

To make the motion mentioned previous section, the crescent-like shape of the trajectory is needed. Statistical analysis of the crescent-like shape of the trajectory was conducted to set the rate of time duration of the upper section of the desired trajectory. A total of 10,000 samples that satisfied the geometrical properties of the crescent-like shape (right side of Fig. 27) were analyzed, and the results are shown as a histogram in Fig. 26. In the histogram, most of the crescent-like shapes of the trajectory exist over 50% of the rate of duration of the upper section. This makes it is hard to find a four-bar linkage where the duration rate of lower section of the trajectory is over 50% and with trajectory similar to the desired trajectory. Therefore, we made the desired trajectory like the right side of Fig. 26. The upper section of the desired trajectory was set the duration rate to be 61 to 65% and increased by 1%.

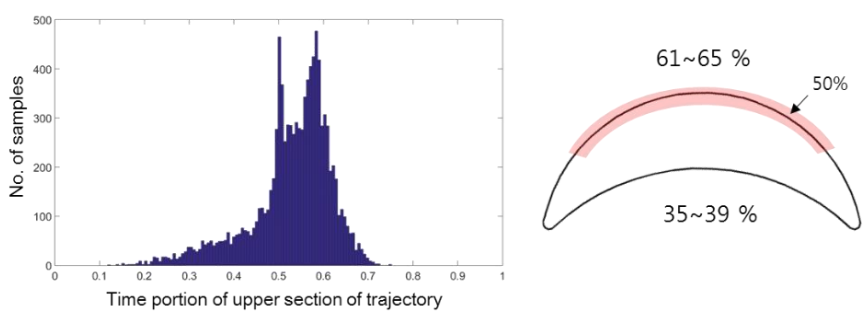

Figure 26 Statistical analysis of crescent-like shape of the trajectory and design objective of the four-bar linkage trajectory

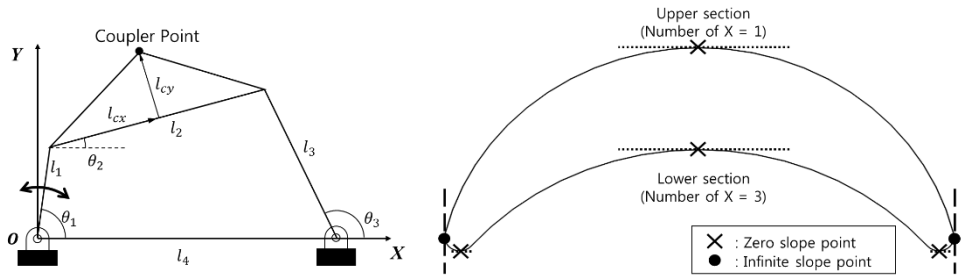

Figure 27(Left) Schematic of four-bar linkage and (Right) crescent-like shape trajectory with geometrical properties

2.2.2 Synthesis of four-bar linkage

Using five desired trajectories, the path synthesis of four-bar linkage is conducted. Because the size of the trajectory is not important, the step 3 of design process (section 2.2 of part 1) was skipped here. Therefore, we set l_1 to 100. The results are shown in Table 13 and show that the difference between the duration rate of the desired trajectory and that of the generated trajectory is increased as the RMS value is increased. Because there are few results to generate the 65% path in the statistical results, the difference between the duration rate of the desired and obtained looks reasonable.

Table 13 The results of path synthesis of four-bar linkage

Design variables	Desired duration rate of upper trajectory				
	61%	62%	63%	64%	65%
l_1	100.0	100.0	100.0	100.0	100.0
l_2	380.0	487.5	478.8	425.0	320.0
l_3	320.0	448.8	497.5	400.0	320.0
l_4	200.0	180.0	171.3	165.0	155.0
l_{cx}	130.0	127.5	185.0	160.0	150.0
l_{cy}	245.0	260.0	195.0	260.0	200.0
θ_0	-0.7510	-0.8764	-1.0530	-0.8578	-0.9756
RMSE value	0.1906	0.1819	0.1739	0.1754	0.3868
Time portion	60.8 %	61.8 %	62.9 %	63.8 %	64.2 %

2.3 Rotational transmission mechanism synthesis

To make the RTM using a four-bar linkage, an output plate that fits well with each four-bar linkage has to be designed. The design process is as follows:

1. Rotate the trajectory of the four-bar linkage to have maximum width (Rotated by θ_0 in Table 13).
2. Find the symmetrical shape in the upper part of the trajectory.
3. Find the vertex point of the isosceles triangle formed by the two points from step 2 in Fig. 28 with an internal angle of $2\pi/14$ (transmission ratio: 7 rev. to 1 rev.).
4. Design the output plate with 14 slits arranged at equal intervals and radius equal to the length of one side of the isosceles triangle.

An example process with the 61% case is demonstrated in Fig. 28. Fig. 29 shows the results for all cases.

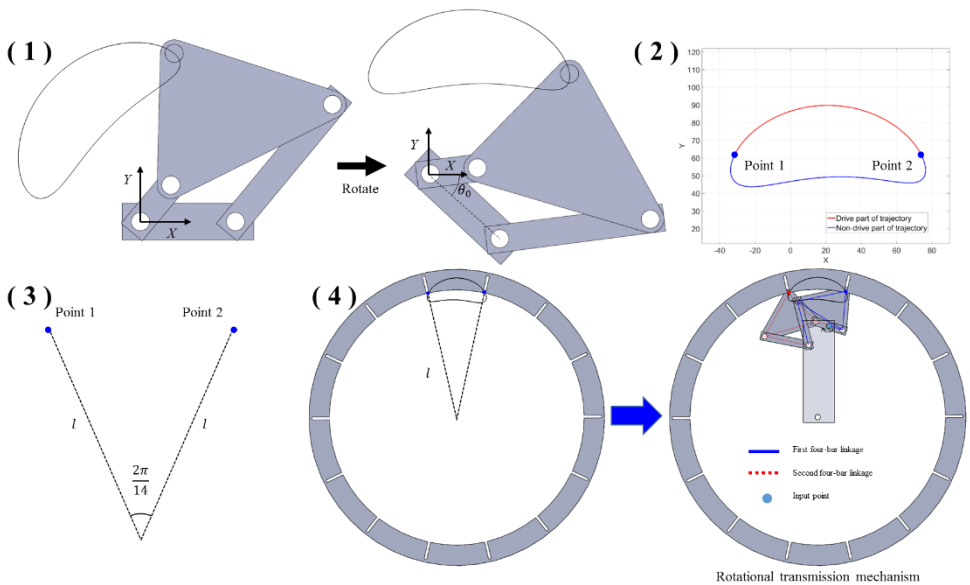

Figure 28 Design procedure of rotational transmission mechanism

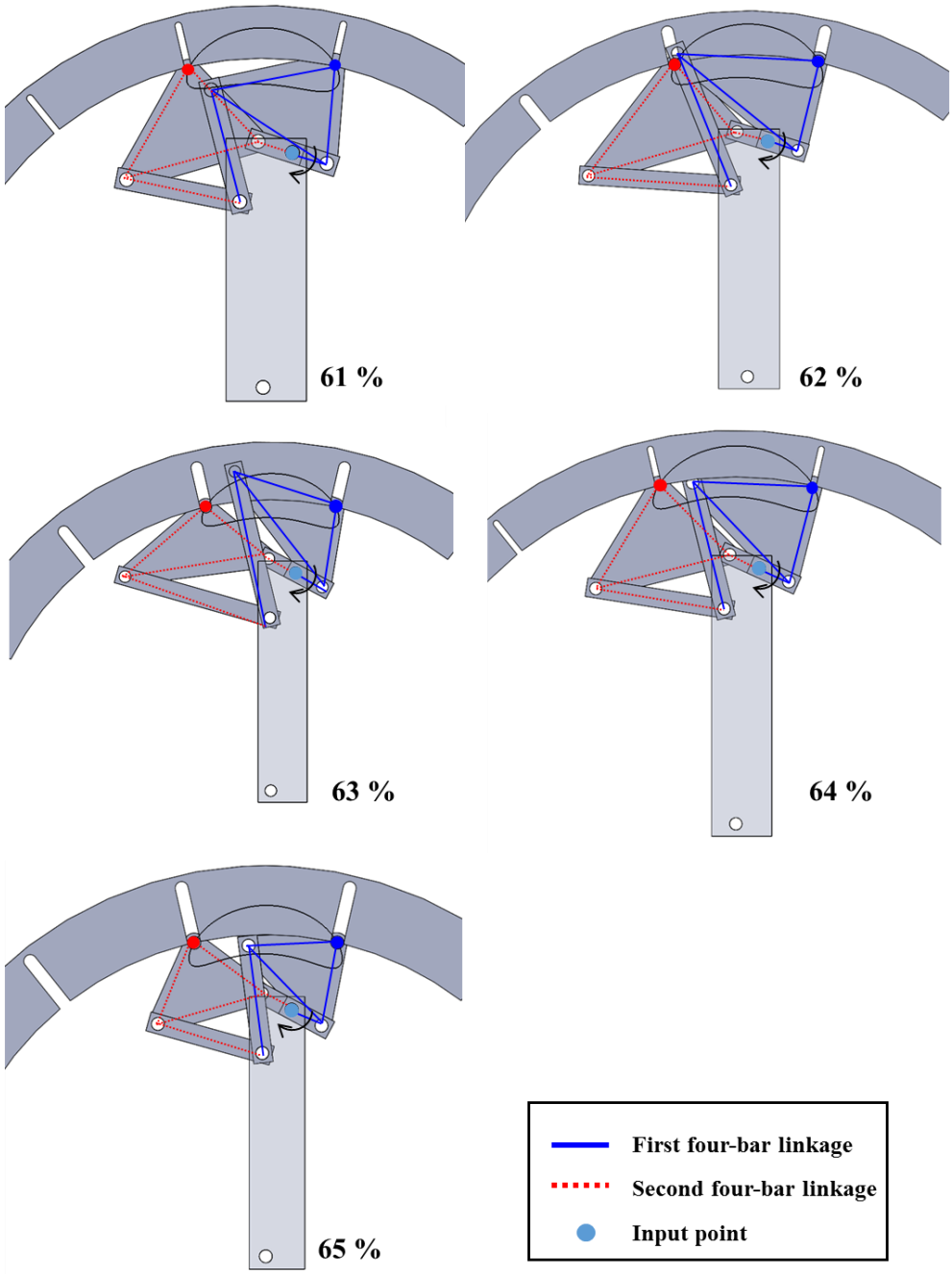

Figure 29 Rotational transmission mechanisms of each case

Chapter 3 Analysis

3.1 Analysis by simulations

To figure out the mechanical performance, motion analysis for each design was conducted. Instead of formulating a dynamic equation, motion analysis using SolidWorks 3D CAD software was conducted. The input velocity is 60 RPM, and the required torque is 1000 N · mm.

The Fig. 30 shows that the angular velocities of each output plate are fluctuated. This is because of the difference of the radius of curvature between the drive part of the four-bar linkage and the output plate. Only 50% of the trajectory drives the output plate, so the radius of curvature should not be the same. Therefore, the fluctuation of the output velocity is inevitable. In order to quantify the fluctuation, the gaps between the maximum and minimum velocity are divided by the average velocity in Table 14. Table 15 shows the corresponding required torque of the four-bar linkage.

Table 14 Fluctuations of angular velocity of output plate

	Average Velocity (rad/sec)	Maximum Velocity (rad/sec)	Minimum Velocity (rad/sec)	Fluctuation
61%	0.9000	1.0691 (18.79% of Avg.)	0.4723 (-47.52% of Avg.)	66.31 %
62%	0.8992	1.0621 (18.11 % of Avg.)	0.4686 (-47.88 % of Avg.)	65.99 %
63%	0.9001	1.0592 (17.68 % of Avg.)	0.4728 (-47.47 % of Avg.)	65.15 %
64%	0.8990	1.0470 (16.46 % of Avg.)	0.5074 (-43.56 % of Avg.)	60.02 %
65%	0.8975	1.0455 (16.50 % of Avg.)	0.5316 (-40.77 % of Avg.)	57.27 %
Gear mechanism	0.8976	0.8976 (0 % of Avg.)	0.8976 (0 % of Avg.)	0 %
Geneva drive	0.8975	4.8155 (436.56 % of Avg.)	0 (-100 % of Avg.)	536.56 %

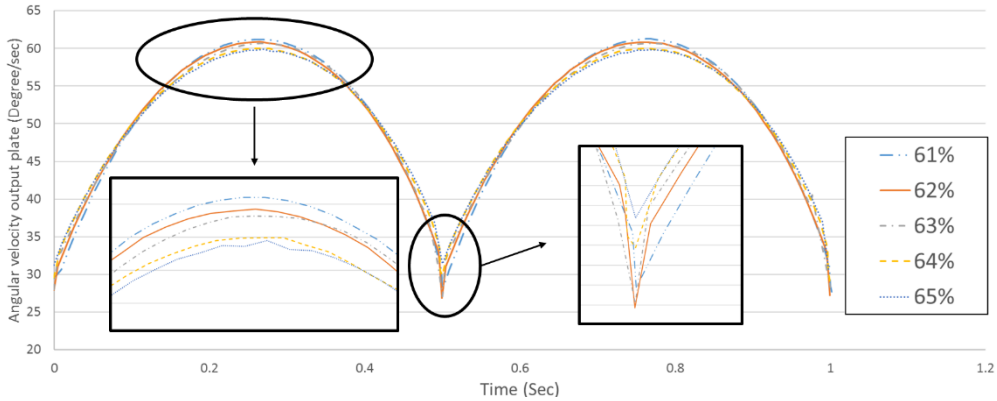

Figure 30 Angular velocity of output plate by simulation

Table 15 Required input torque of four-bar linkage

	Average Torque (N·mm)	Maximum Torque (N·mm)	Minimum Torque (N·mm)	Fluctuation
61%	145.373	175.016 (20.39 % of Avg.)	77.691 (-46.55 % of Avg.)	66.95 %
62%	144.71	189.877 (31.21 % of Avg.)	79.582 (-45.01 % of Avg.)	76.22 %
63%	147.585	191.537 (29.78 % of Avg.)	70.233 (-52.41 % of Avg.)	82.19 %
64%	146.192	189.206 (29.42 % of Avg.)	76.713 (-46.80 % of Avg.)	76.95 %
65%	145.194	184.842 (27.31 % of Avg.)	59.23 (-59.21 % of Avg.)	86.51 %
Gear mechanism	142.86	142.86 (0 % of Avg.)	142.86 (0% of Avg.)	0 %
Geneva drive	149.01	837.94 (462.32 % of Avg.)	0 (-100 % of Avg.)	562.32 %

3.1 Singularity based design selection

Throughout the simulation, the results show that the angular velocity of output plate and required torque are fluctuated. As the time portion of the upper side of trajectory increased(61% → 65%), the fluctuation of angular velocity is decreased. On the other hand, that of the required torque is increased. Thus, it is hard to determine the final design of the four-bar linkage as the RTM. Therefore, in this dissertation, the final design is determined by the singular point analysis.

In the ideal situation of manufacture and assembly, if the four-bar linkage satisfy some constraints such as grashof condition, the singularity doesn't occur. On the other hand, in the real world situation, due to the tolerance of the manufacture

and assembly, there is a possibility to occur the singularity. In case of crank-rocker four-bar linkage, the possibility of occurring the singularity is increased, as the minimum value of the θ_4 (see the Appendix 1) is decreased. This values are calculated as follows:

$$Minimum\ \ of\ \ \theta_4 = \cos^{-1}\frac{{l_2}^2 + {l_3}^2 - (l_4 - l_1)^2}{2l_2 l_3}$$

Table 16 shows the minimum of θ_4 according to the time portion of the upper side of trajectory. The table shows that 61%-time portion of upper trajectory case is the best option to the final design.

Table 16 Minimum values of θ_4

Time portion of upper trajectory	Minimum value of θ_4
61%	13.174
62%	8.585
63%	8.084
64%	8.345
65%	9.860

Chapter 4 Prototyping & Experiment

4.1 Prototyping

From the analysis, the design that 61%-time portion of upper trajectory is selected to prototype. Therefore, the non-servo motor type ATC is designed with that four-bar linkage. The ATC is adopted to the UT280 tapping machine made by the UGINT corporation demonstrated in Fig. 32. The operating principles are shown in Fig. 31.

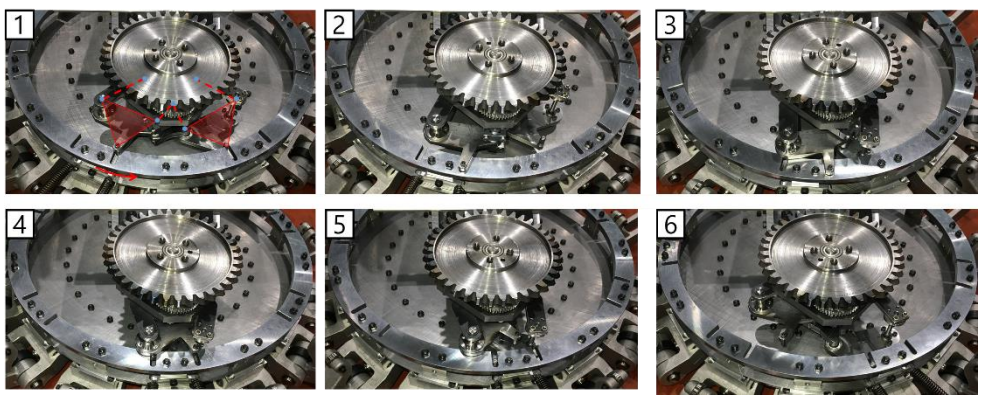

Figure 31 The prototype of the RTM for the automatic tool changer. Posture during (1-6) counterclockwise motion

Figure 32 The prototype of ATC using RTM

4.2 Experiment and Results

Two kinds of experiments were conducted. The first is to ascertain whether a continuous rotation is possible. The input velocity is 60 RPM which is same as

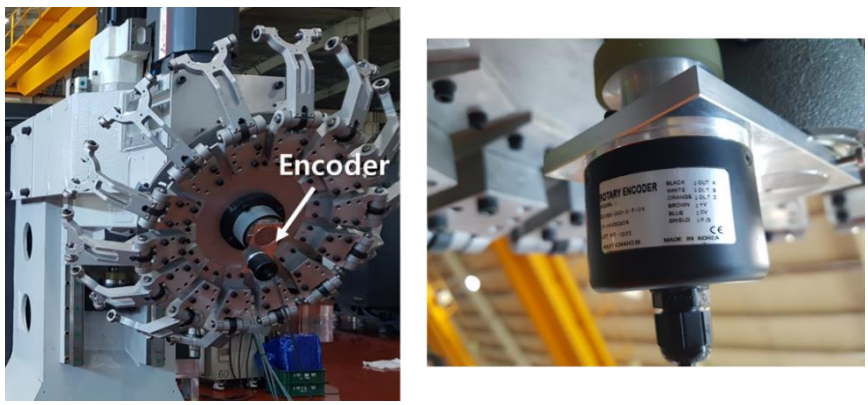

Figure 33(Left) The experimental environment and (Right) Rotary encoder to measure an angular velocity of output plate

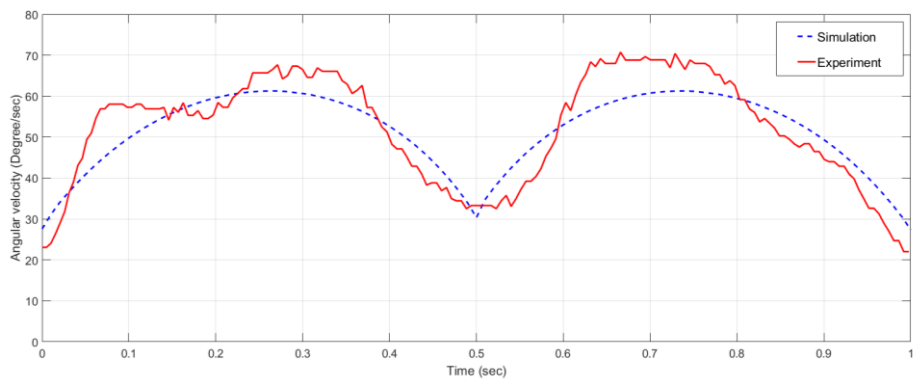

Figure 34 The angular velocity of output plate

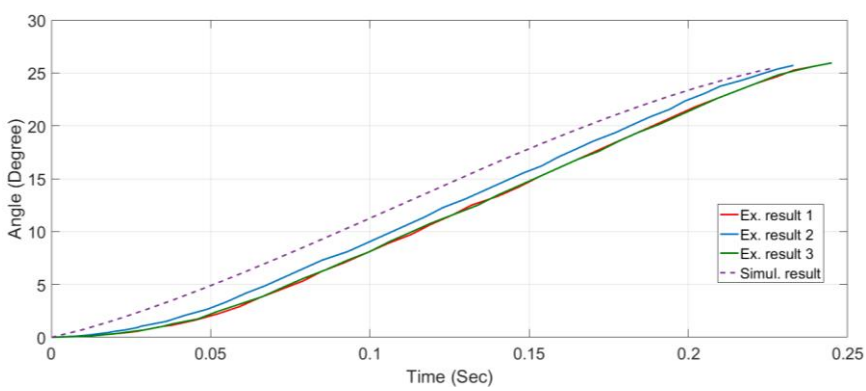

Figure 35 The angle of the output from the second experiment

analysis section. The experimental environment is demonstrated in Fig. 33, and the result is depicted in Fig. 34. The graph shows that the angular velocity of the output plate rotates similar to the analysis result. However, the vibrations are observed in some sections. This is not a critical impact to the device. However, the research to reduce of vibration will be conducted near future. The second is to measure the time of rotation of next tool (1/14 rotation of ATC). To achieve a rotational time less than or equal to 0.25 sec the input 1/2 rotation with 130 RPM of main spindle is applied. The experimental environment is same as the first experiment. Fig. 35 demonstrated the results of the second experiment. From the second experiment, it was confirmed that the proposed mechanism can rotate ATC to the next tool within 0.25 sec. Because this time is faster than that of conventional ATC, I think that the proposed mechanism has a possibility as a product.

Chapter 5 Discussion & Conclusion

This part has presented a new rotational transmission design and its synthesis. The new rotational transmission mechanism is a device for continuously rotating the output plate using two four-bar linkages. There already exist a mechanism using single four-bar linkage. However, the existing mechanism is only for the intermittent rotating output motion. Therefore, the mechanism proposed in this paper is totally different from the existing mechanism. The design method is also different. In case of the RTM using single four-bar linkage, the trajectory of coupler point, that drives the output plate, of four-bar linkage is the only to be considered in design methodology. However, in the case of using two four-bar linkage in the RTM for the continuous rotational motion, both the trajectory and the position of the coupler points have to be considered at the same time in order for the one four-bar linkage to start contacting with output plate as soon as the other four- bar linkage loses contact with output plate. To doing this, the method developed in the part 1 was adopted.

From the statistical analysis, the target trajectory was set as a crescent-like shape. The time portions of upper part of crescent-like shape were set to be 61% ~ 65% of whole cycle time. A total of five cased of four-bar linkage were designed. Then, output plates that matched each four-bar linkage were designed.

Instead of formulating a dynamic equation, a dynamic simulation using 3D CAD software was conducted. The results showed that the angular velocity of the output plate fluctuated by 57 to 66 % of the average velocity. The case with 65% duration rate of the upper trajectory had the minimum fluctuation among the five cases. The average required torques to output 1000 N·mm at the output plate showed an opposite pattern. The fluctuation of torque was 66 to 86% of the average torque. The 61% case had the minimum fluctuation. Because the hardness of the selection among the five cases. The singularity analysis conducted to determine the final design selection. From the singularity analysis, the 61% case selected as a four-bar linkage of the rotational transmission mechanism for non-servo motor ATC.

The prototype of rotational transmission mechanism for non-servo motor ATC was made and applied to the real product called UT280 made by UGINT corporation. Two experiments (60 RPM continuous rotation and 130 RPM with 0.5 rotation) were

conducted to verify the feasibility of the mechanism. The result shows that the device works well. However, the further study to reduce the vibration of the output plate is required.

Conclusions and future works

In this study the methodology for the design of four-bar linkage was presented. The method is composed of 3 steps. In the first step, checking the generated trajectory is whether or not belongs to the desired target shape of trajectory. To doing this, the hypothesis, that the shapes of trajectory of crank-rocker four-bar linkage are classified into four-type, was set and verified by two methods. One is visual inspection and the other one is simulation. Once generated trajectory pass the first step, the next step is to calculate the root-mean-square error of the 1st order derivative (slope) between generated and desired trajectory. If the RMSE value of the second step is optimized, the shapes of the generated and desired trajectory are on the similar. The reason for this was proved in this dissertation. In the final step, the size of the trajectory is optimized by minimizing RMSE of 2nd order derivative (change in angle of slope) between generated and desired trajectory. If the RMSE value of the third step is optimized, the sizes of the generated and desired trajectory are the same. The reason for this was also proved in this dissertation.

The optimization algorithm for the design method was also presented in this dissertation. The algorithm called hybrid Taguchi-random coordinate search algorithm (HTRCA). The HTRCA combines two method called Taguchi method, which is famous as robust design method based on experimental data, and the random coordinate search algorithm, which can find an optimal point by optimizing a function value along one direction generated randomly one at a time. Seven test functions were used to verify the robustness and effectiveness of the HTRCA. In addition, the verification to apply for path synthesis of four-bar linkage was conducted. Despite, HTRCA cannot achieve the best optimal solution in overall cases, the method can find the reasonable optimal solutions compared to the other single evolutionary algorithms and hybrid algorithm such as genetic algorithm, particle swarm optimization, differential evolution and GA–DE hybrid algorithm. Therefore, I saw the possibility to adopt the developed algorithm to a tool for design methodology of four-bar linkage.

The proposed design methodology using HTRCA was also verified. To validate the method, lots of simulation cases were presented. The simulation cases showed that the proposed path synthesis can get the better optimal solution compare to the conventional method.

This dissertation also presents a practical application of the proposed design

methodology. That is a rotational transmission mechanism for non-servo motor automatic tool changer using dual four-bar linkage. The new rotational transmission mechanism is a device for continuously rotating the output plate using two four-bar linkages. Throughout some analysis the prototype of the rotational transmission mechanism was made. The experiment result shows that the device worked well. The further study to reduce the vibration of output plate is required.

The design methodology of this dissertation could be used in many engineering problems, that considering the velocity of the trajectory, ever didn't solve. Also, the concept of the method, that using 1^{st} and 2^{nd} derivative of the trajectory, could be adopted to the path synthesis of other linkage such as six bar linkage.

Bibliography

1. Norton, R. L., Design of machinery: an introduction to the synthesis and analysis of mechanisms and machines, McGraw-Hill Professional, p.117, 2004.
2. Four-bar linkage, (2010, October, 29), Retrived from https://en.wikipedia.org /wiki/Four-bar_linkage.
3. J.A. Hrones, Analysis of the Four-Bar Linkage, Published Jointly by the technology Press of the Massachusetts Institute of Technology, and Wiley, 1951.
4. Sandor, G. N., A general complex-number method for plane kinematic synthesis with applications (Doctoral dissertation, Columbia University.), 1959.
5. C.Y. Han, A general method for the optimum design of mechanisms, J. Mech. 1 (3) (1967) 301–313.
6. R. Sancibrian, F. Viadero, P. Garcıa, A. Fernández, Gradient-based optimization of path synthesis problems in planar mechanisms, Mech. Mach. Theory 39 (8) (2004) 839–856.
7. W.Y. Lin, A GA–DE hybrid evolutionary algorithm for path synthesis of four-bar linkage, Mech. Mach. Theory 45 (8) (2010) 1096–1107.
8. R. Zbikowski, C. Galinski, C.B. Pedersen, Four-bar linkage mechanism for insectlike flapping wings in hover: concept and an outline of its realization, J.Mech. Des.127 (4) (2005) 817–824.
9. J.S. Zhao, Z.F. Yan, L. Ye, Design of planar four-bar linkage with n specified positions for a flapping wing robot, Mech. Mach. Theory 82 (2014) 33–55.
10. C. Zhang, R.L. Norton, P.E ., T. Hammonds, Optimization of parameters for specified path generation using an atlas of coupler curves of geared five-bar linkages, Mech. Mach. Theory 19 (6) (1984) 459–466.
11. A.G. Erdman, G.N. Sandor, S. Kota, Mechanism Design: Analysis and Synthesis (Vol. 1), Prentice-Hall, Englewood Cliffs, 1984.
12. Uicker, J. J., Pennock, G. R., & Shigley, J. E., Theory of machines and mechanisms (p. 466). Oxford: Oxford University Press, 2011.
13. A.G. Erdman, Three and four precision point kinematic synthesis of planar linkages, Mech. Mach. Theory 16 (3) (1981) 227–245.
14. C.W. Wampler, A.P. Morgan, A.J. Sommese, Complete solution of the nine-point path synthesis problem for four-bar linkages, J. Mech. Des. 114 (1) (1992) 153–159.
15. J. Chu, W. Cao, Synthesis of coupler curves of planar four-bar linkages through fast fourier transform, Chin. J. Mech. Eng. 29 (5) (1993) 117–122.

16. J.R. McGarya, Rapid search and selection of path generating mechanisms from a library, Mech. Mach. Theory 29 (2) (1994) 223–235.

17. I. Ullah, S. Kota, Optimal synthesis ofmechanisms for path generation using Fourier descriptors and global searchmethods, J.Mech. Des. 119 (4) (1997) 504–510.

18. S. Krishnamurty, D.A. Turcic, Optimal synthesis of mechanisms using nonlinear goal programming techniques, Mech. Mach. Theory 27 (5) (1992) 599–612.

19. J.A. Cabrera, A. Simon, M. Prado, Optimal synthesis of mechanisms with genetic algorithms, Mech. Mach. Theory 37 (10) (2002) 1165–1177.

20. D.A. Hoeltzel, W.H. Chieng, Pattern matching synthesis as an automated approach to mechanism design, J. Mech. Des. 112 (2) (1990) 190–199.

21. J.M. McCarthy, G.S. Soh, Geometric Design of Linkages, 11Springer, 2010.

22. F. Freudenstein, Design Of Four-Link MechanismsPh. D. Thesis Columbia University, USA, 1954.

23. D.R. Jones, M. Schonlau, W.J. Welch, Efficient global optimization of expensive black-box functions, J. Glob. Optim. 13 (4) (1998) 455–492.

24. L.M. Rios, N.V. Sahinidis, Derivative-free optimization: a review of algorithms and comparison of software implementations, J. Glob. Optim. 1-47 (2011).

25. J.T. Tsai, T.K. Liu, J.H. Chou, Hybrid Taguchi-genetic algorithm for global numerical optimization, IEEE Trans. Evol. Comput. 8 (4) (2004) 365–377.

26. Y.T. Kao, E. Zahara, A hybrid genetic algorithm and particle swarm optimization for multimodal functions, Appl. Soft Comput. 8 (2) (2008) 849–857.

27. J.A. Cabrera, A. Simon, M. Prado, Optimal synthesis of mechanisms with genetic algorithms, Mech. Mach. Theory 37 (10) (2002) 1165–1177.

28. S.K. Acharyya, M. Mandal, Performance of EAs for four-bar linkage synthesis, Mech. Mach. Theory 44 (9) (2009) 1784–1794.

29. F. Penunuri, R. Peón-Escalante, C. Villanueva, D. Pech-Oy, Synthesis ofmechanisms for single and hybrid tasks using differential evolution, Mech.Mach. Theory 46 (10) (2011) 1335–1349.

30. W.L. Goffe, G.D. Ferrier, J. Rogers, Global optimization of statistical functions with simulated annealing, J. Econ. 60 (1) (1994) 65–99.

31. A. Sardashti, H.M. Daniali, S.M. Varedi, Optimal free-defect synthesis of four-

bar linkage with joint clearance using PSO algorithm, Meccanica 48 (7) (2013)1681–1693.

32. W.Y. Lin, A GA–DE hybrid evolutionary algorithm for path synthesis of four-bar linkage, Mech. Mach. Theory 45 (8) (2010) 1096–1107.

33. G.S. Peace, Taguchi Methods: a Hands-on Approach, Addison-Wesley, Wokingham, England, 1993 23–311.

34. J.C. Bezdek, R.J. Hathaway, R.E. Howard, C.A. Wilson, M.P. Windham, Local convergence analysis of a grouped variable version of coordinate descent, J. Optim. Theory Appl. 54 (3) (1987) 471–477.

35. G. Taguchi, Introduction to Quality Engineering: Designing Quality Into Products and Processes White Plains, Kraus International Publications, NY, 1986.

36. P.J. Ross, Taguchi Techniques for Quality Engineering, McGraw-Hill, New York, 1988.

37. C. Li, R. Priemer, K.H. Cheng, Optimization by random search with jumps, Int. J. Numer. Methods Eng. 60 (7) (2004) 1301–1315.

38. A.V. Levy, A. Montalvo, The tunneling algorithm for the global minimization of functions, SIAM J. Sci. Stat. Comput. 6 (1) (1985) 15–29.

39. S. Lucidi, M. Piccioni, Random tunneling by means of acceptance-rejection sampling for global optimization, J. Optim. Theory Appl. 62 (2) (1989) 255–277.

40. J.A. Nelder, R. Mead, A simplex method for function minimization, Comput. J. 7 (1964) 308–313.

41. S. Dibakar, T.S. Mruthyunjaya, Synthesis of workspaces of planar manipulators with arbitrary topology using shape representation and simulated annealing, Mech. Mach. Theory 34 (3) (1999) 391–420.

42. H. Zhou, E.H. Cheung, Optimal synthesis of crank–rocker linkages for path generation using the orientation structural error of the fixed link, Mech. Mach. Theory 36 (8) (2001) 973–982.

43. Kim, J. Design and Analysis of a Lizard-Inspired Legged Robot, Ph. D. Seoul national University, South Korea, 2015.

44. D. J. Irschick, & B. C. Jayne, Comparative three-dimensional kinematics of the hindlimb for high-speed bipedal and quadrupedal locomotion of lizards. Journal of Experimental Biology, 202(9), (1999) 1047-1065

45. Nariman-Zadeh, N., Felezi, M., Jamali, A., & Ganji, M. (2009). Pareto optimal synthesis of four-bar mechanisms for path generation. Mechanism and Machine Theory, 44(1), 180-191.

46. Matekar, S. B., & Gogate, G. R. (2012). Optimum synthesis of path generating four-bar mechanisms using differential evolution and a modified error function. Mechanism and Machine Theory, 52, 158-179.

47. Fujimoto, A., & Sato, N. (2007). U.S. Patent No. 7300393. Washington, DC: U.S. Patent and Trademark Office.

48. Dijksman, E. A. (1966). Jerk-free Geneva wheel driving. Journal of Mechanisms, 1(3-4), 235IN1281-280IN2283.

49. Erdman, A. G., & Sandor, G. N. (1997). Mechanism design: analysis and synthesis (Vol. 1). Prentice-Hall, Inc..

Appendix 1
Coupler point of crank-rocker four-bar linkage

To form a crank-rocker four-bar linkage, the relationships between each link length need to satisfy the Grashof conditions [21]:

$$T_1 = l_4 + l_2 - l_1 - l_3 > 0 \quad \text{(A1a)}$$

$$T_2 = l_3 + l_4 - l_1 - l_2 > 0 \quad \text{(A1b)}$$

$$T_3 = l_3 + l_2 - l_1 - l_4 > 0 \quad \text{(A1c)}$$

Each variable can be found in Fig. A1. If the input link (l_1) rotates once, a coupler curve is generated that is the same as the trajectory of the coupler point of the four-bar linkage. Fig. A1 shows the position of coupler point C on a four-bar linkage, which is described as follows:

$$C_x = l_1 \cos(\theta_1 + \theta_0) + l_{cx} \cos(\theta_2 + \theta_0) - l_{cy} \sin(\theta_2 + \theta_0) \quad \text{(A2a)}$$

$$C_y = l_1 \sin(\theta_1 + \theta_0) + l_{cx} \sin(\theta_2 + \theta_0) + l_{cy} \cos(\theta_2 + \theta_0) \quad \text{(A2b)}$$

Because the four-bar linkage has one degree of freedom, the angle θ_2 can be represented by the input angle θ_1. Freudestein's equation was used to determine the relationship between θ_2 and the input angle [22]:

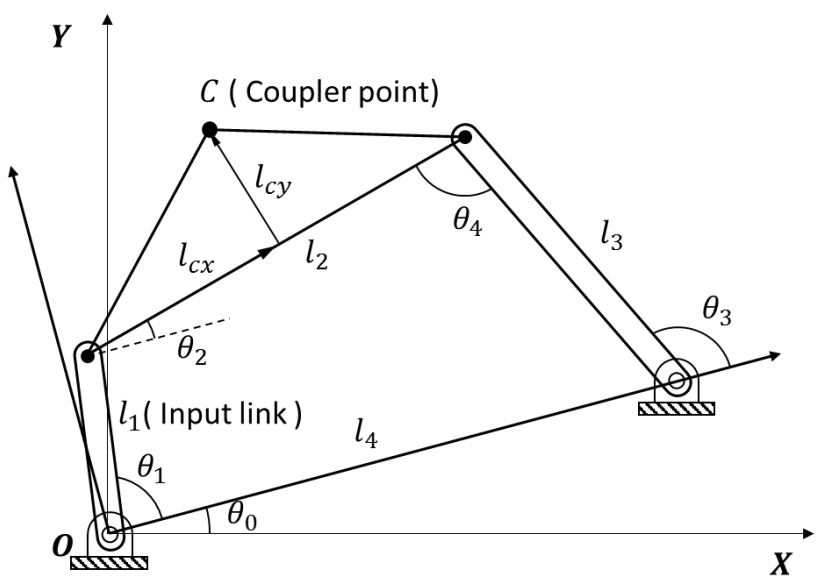

Figure A1 Four-bar Linkage mechanism in a global coordinate system

Appendix

$$K_1 \cos\theta_3 - K_2 \cos\theta_1 + K_3 = \cos(\theta_1 - \theta_3) \quad \text{(A3a)}$$

$$K_1 \cos\theta_2 - K_4 \cos\theta_1 + K_5 = \cos(\theta_1 - \theta_2) \quad \text{(A3b)}$$

where

$$K_1 = \frac{l_4}{l_1}, K_2 = \frac{l_4}{l_3}, K_3 = \frac{{l_1}^2 - {l_2}^2 + {l_3}^2 + {l_4}^2}{2 l_1 l_3}, K_4 = \frac{l_4}{l_2}, K_5 = \frac{{l_3}^2 - {l_4}^2 - {l_1}^2 - {l_2}^2}{2 l_1 l_2}.$$

From equations (A3a) and (A3b), the solutions of θ_2 and θ_3 regarding the input angle θ_1 are obtained as follows:

$$\theta_2 = 2\tan^{-1}\left\{\left(-B \pm \sqrt{B^2 - 4AC}\right)/2A\right\} \quad \text{(A4a)}$$

$$\theta_3 = 2\tan^{-1}\left\{\left(-E \pm \sqrt{E^2 - 4EF}\right)/2D\right\} \quad \text{(A4b)}$$

where

$$A = \cos\theta_1 - K_1 + K_4 \cos\theta_1 + K_5$$

$$B = -2\sin\theta_1$$

$$C = K_1 + (K_4 - 1)\cos\theta_1 + K_5$$

$$D = \cos\theta_1 - K_1 + K_2 \cos\theta_1 + K_3$$

$$E = -2\sin\theta_1$$

$$F = K_1 - (K_2 + 1)\cos\theta_1 + K_3$$

Substituting equation (A4a) into equations (A2a) and (A2b) allows for the derivation of the coupler point position of a four-bar linkage using a single variable in the range of [0 2π].

Abstract in Korean

4절링크는 매우 다양하게 사용되는 기계장치 중에 하나이다. 4절링크는 필름 영사기 구조에 사용되어 필름을 이동하는 동력전달 장치로 사용되는 가하면, watt's 링키지와 같은 기계적인 구조로도 사용된다. 입력이 회전운동임에도 불구하고 출력이 다양한 모양의 움직임이 가능하기 때문에 매우 다양한 곳에 사용된다. 그럼에도 불구하고, 목표 궤적이 주어져 있을 때 이를 잘 추종하는 4절링크를 설계하는 방법론에 대한 연구는 매우 제한적이다. 본 학위 논문에서는 목표 궤적의 모양과 속도를 잘 추종하는 4절링크 설계 방법론을 제시한다.

본 학위논문은 2개의 파트로 구성되어있다. 첫 번째 파트는 목표 궤적과 모양과 속도가 유사한 4절링크를 설계하는 방법론에 대한 것이다. 두 번째 파트는 실용적인 적용 사례에 대한 것이다. 첫 번째 파트에서 제시하는 4절링크 설계 방법론은 크게 3가지 단계로 이루어져있다. 첫 번째 단계에서는 생성된 궤적의 모양이 목표 궤적이 속한 궤적의 모양 카테고리에 속하는지 확인하는 단계이다. 본 학위논문에서는 크랭크-라커 4절링크의 궤적이 총 4가지로 분류 될 수 있을 것이라 가정하였고, 이를 증명하였다. 첫 번째 단계를 통과하면, 두 번째 단계에서는 궤적의 모양을 결정한다. 궤적의 모양은 목표 궤적과 생성 궤적의 시간에 따른 1계 미분의 차의 RMSE를 최소화 하면 얻어진다. 그리고 마지막 단계에서는 목표 궤적과 생성 궤적의 시간에 따른 2계 미분의 차의 RMSE를 최소화 하여, 궤적의 최종적인 크기를 결정한다. 이러한 새로운 접근방법은 3가지 강점을 가지고 있다. 첫 번째는 목표 궤적이 연속적이며 폐곡선의 형태 여도 적용 가능하다. 두 번째는 궤적의 모양 카테고리를 이용하기 때문에, 최종적으로 얻은 결과물이, 의도하지 않은 형상을 가지는 경우가 발생하지 않는다. 마지막으로는 시간에 따른 미분 값을 사용하므로 목표 궤적의 각 영역별 시간 또는 속도를 고려한 설계를 수행할 수 있다.

본 연구에서 개발한 궤적생성알고리즘은 수치 해석적 방법론이다. 따라서 각 링크의 링크 길이를 찾아내는 데에는 최적화 알고리즘이 필요하다. 본 연구에서는 새로운 하이브리드 최적화 알고리즘 또한 제시한다. 최적화 알고리즘은 Hybrid Taguchi-random coordinate search algorithm(HTRCA)라 불린다. HTRCA는 다구치 방법론(Taguchi method, TM)과 random coordinate search(RCA)알고리즘을 결합한 최적화 방법론이다. RCA는 한 개의 변수를 임의의 순서로 다양한 방향과 간격으로 변형해 보면서 최적 값을 찾는 알고리즘이다. RCA가 한 번에 한 개의 변수를 변경하기 때문에, RCA의 결과는 초기 값에 민감한 경향을 가진다. 여기에서 TM을 이용해 최적 값에 근접한 결과를 얻은 후에 이를 초기 값으로 RCA를 사용하는 방식이 HTRCA의 최적 값을 찾는 방식이다. TM은 한번에 2개 이상의 변수를 변경하면서, 초기 값 뿐만 아니라, 국소 최적 점(local minimum point)을 탈출하는 데에도 사용된다. 이렇게 두 가지 알고리즘을 결합함으로써, 최적 값을 매우 효율적으로 찾을 수 있다. 7개의 함수를 통해서 다른 알고리즘대비 견실하고 효율적으로 최적 값을 찾을 있음을 보였다. 마지막으로 기존의 4절링크 설계 방법론에 적용을 하여 이전에 수행되었던 연구와의 결과 비교를 수행하였다.

새로운 4절링크 설계 방법론을 검증하기 위해서 goodness of traceability라는 새로운 지표를 정의하고 3가지 사례연구를 수행하였다.

본 학위논문의 두 번째 파트는 실용적인 연구에 적용하는 사례에 대한 것이다. 그것은 태핑머신의 자동공구교환장치용 회전 변환 장치이다. 본 연구에서 개발한 회전 변환 장치는 두개의 4절링크를 이용한다. 한 개한 4절링크가 출력판과 접촉을 시작하면, 다른 4절링크는 접촉을 잃는다. 이러한 방식으로 출력판은 연속적으로 회전 할 수 있다. 제시된 메커니즘은 한 개의 4절링크를 이용한 방식과는 완전히 다르다. 한 개의 4절

링크를 이용하는 방식을 설계할 때는 오직 궤적의 모양만이 중요하다. 하지만, 두개의 4절링크를 이용하게 되면, 궤적의 모양뿐만 아니라 속도까지도 중요한 요인이 된다. 이 파트에서는 첫 번째 파트에서 개발한 4절링크 설계 방법론을 사용하였다. 설계는 기구학해석과 특이점 해석을 통해 진행되었다. 동역학 시뮬레이션을 수행하고, 프로토타입을 제작하여 실제 동작성을 검증해보았다. 그리고 마지막으로는 태핑머신에 적용해보았다. 이러한 연구를 통해서 본인은 새롭게 개발한 4절링크 설계 방법론이 목표 궤적이 주어진 4절링크 다양한 공학적 설계 문제에 적용될 수 있음을 확인하였다.